AD-A115 468 SPERRY RESEARCH CENTER SUDBURY MA F/G 9/5
MULTIPOLE MONOLITHIC SURFACE ACOUSTIC WAVE (SAW) RESONATOR FILT--ETC(U)
APR 82 N00014-81-C-2066
UNCLASSIFIED SRC-CR-82-19 NL

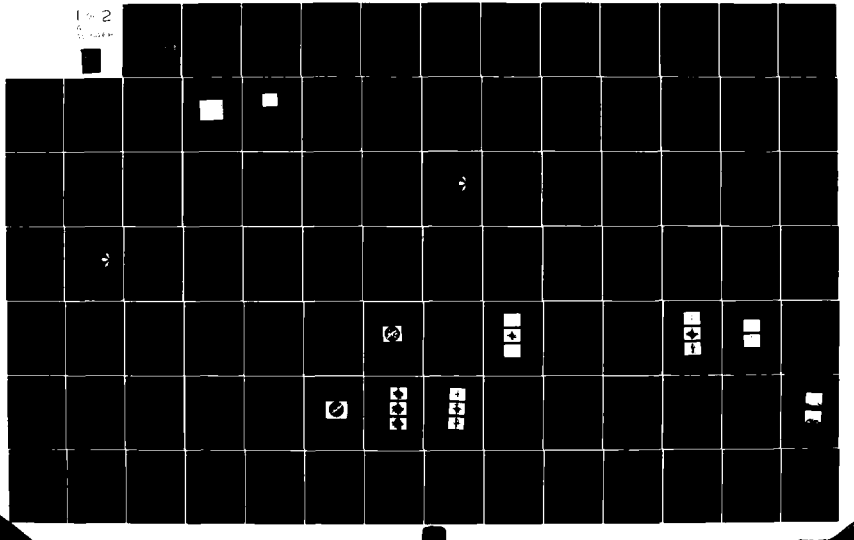

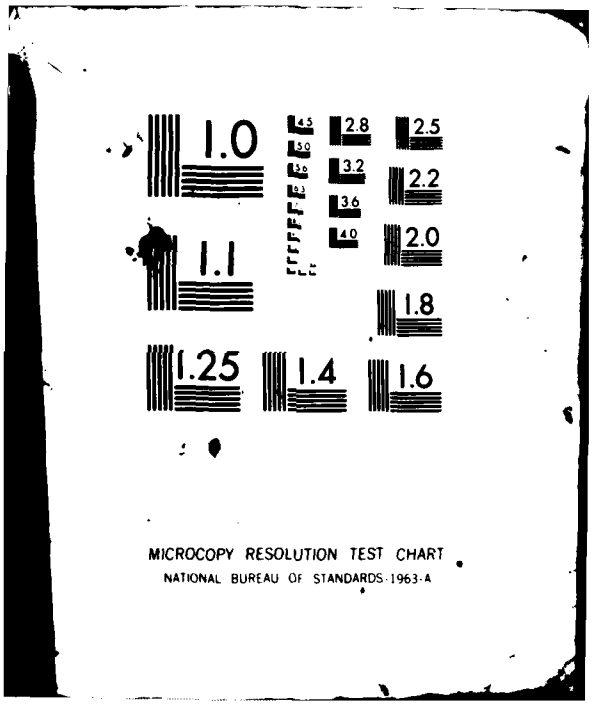
1.0
1.1
1.25
1.4
1.6
2.8
3.2
3.6
4.0
2.5
2.2
2.0
1.8
MICROCOPY RESOLUTION TEST CHART
NATIONAL BUREAU OF STANDARDS-1963-A

MULTIPOLE MONOLITHIC SURFACE ACOUSTIC WAVE (SAW) RESONATOR FILTERS

Interim Technical Report
Contract No. N00014-81-C-2066

SRC-CR-82-19
April 1982

Prepared by
Sperry Research Center
100 North Road
Sudbury, MA 01776

Prepared for
Naval Research Laboratory
Washington, DC 20375

TABLE OF CONTENTS

LIST OF ILLUSTRATIONS

LIST OF ILLUSTRATIONS (Continued)

LIST OF ILLUSTRATIONS (Continued)

SECTION 1
INTRODUCTION

In this interim report we discuss the work which we have performed and the results achieved in our effort to produce high performance multipole surface-acoustic-wave (SAW) resonator filters. This report covers the first year of a two-year effort in which we are attempting to design and fabricate filters meeting the specifications in Table I below.

Table I
Filter Specifications

	Type I	Type II
Passband Center Frequency (F_r)	217 MHz	150 MHz
3dB Bandwidth (ΔF_3)	40 kHz (Q_f = 5400)	37 kHz (Q_f = 4050)
Shape Factor (60dB / 3dB)	4/1	8.1/1
Maximum Insertion Loss	10 dB	6 dB
Filter Response	Butterworth	Chebychev (0.5dB ripple)
Minimum Rejection beyond		
$F_R \pm 0.15$ MHz		60 dB
$F_R \pm 0.5$ MHz		80 dB
$F_R \pm 5.0$ MHz		110 dB
Package Size		Minimum Possible
Input/Output Impedance	50 ohms	50 ohms
Operational Temperature Range	10 to 40°C	-10 to 80°C
Filter-to-Filter Phase Difference	10° (over 3 dB bandwidth)	

The goal of this program is to advance the state-of-the-art in multipole SAW resonator technology by building on fundamental knowledge currently available on single-pole SAW resonators, general multipole filter design, and multipole SAW resonators. The method for accomplishing this is the development and small scale production of the two high performance filter designs specified in Table I.

During this first year we have investigated two synthesis procedures[1,2], and we have selected that developed by Matthaei[2] as being completely acceptable and straightforward to use. Reflectors and transducers were chosen as the cavity coupling mechanisms, in various combinations, and the recessed-aluminum-transducer/etched-groove-reflector configuration has been selected for use. We have adapted previously existing resonator analysis computer programs for use in analyzing and

making small adjustments (tweeking) in the synthesized designs. Photomasks have been made and devices fabricated and tested for several designs. Five copies of each of the two filter types have been fabricated and sent to the Naval Research Laboratory for evaluation. The results attained thus far include the successful fabrication of four and six-pole filters meeting many of the specifications. More work is necessary, however, to meet all the requirements.

In the sections which follow we discuss details of the synthesis and analysis procedures, device fabrication, and experimental results. The concluding section contains a summary of the results attained to date, and recommendations for work in the remainder of the program.

SECTION 2
FILTER DESIGN: SYNTHESIS AND ANALYSIS

The steps in filter design are to establish the minimum number of resonant cavities (poles) theoretically required to provide the desired response, selection of the cavity-coupling mechanism for each pair of poles, synthesis of the component sizes (reflectors, transducers, capacitors, and inductors), and analysis and tweeking of the design to ensure the specifications are met when second order effects and various losses are included. The procedures we have developed or implemented we consider to be highly successful in that the synthesis is rapid, being performed in a matter of a hours, and accurate as indicated by the minor amount of tweeking required during analysis. Each step in the design process is outlined below with details for the two designs used for the filters which were delivered. For reference purposes each design is assigned a number which corresponds to our internal (Sperry Research) mask number sequence, and a specific device is numbered with the design number followed one or more digits. For instance, the fourth device made using design D277 is numbered D277-4.

The number of poles required to meet the specification of the Type I and Type II filter were determined from data available in Refs. 4 and 5. For the Type I filter the shape factor is 4/1, and the Butterworth attenuation characteristics presented on Curve 1, Page 82 of Reference 4 (Ω=4), show that a minimum of five poles (n = 5) are required to attain 60 dB rejection for the given shape factor. For the Type II filter with a shape factor of 8.1/1, Curve 7, Page 88 of Ref. 5 (Ω = 8.1) shows that a minimum of three poles (n = 3) are required to attain 60 dB rejection level. For both filter types, the theoretical attenuation is only slightly larger than the 60 dB required. A three-pole (transducer-coupled) Type II filter was designed and fabricated, and we found that the actual shape factor was larger than required. Thus we decided to use four poles for the Type II design and six poles for the Type I filters. The additional cavity for each design did not cause difficulty in any way and ensured that the required shape factor would be attained.

The "ST"-X (42.75° rotated Y) cut of quartz was selected for its thermal stabililty in the neighborhood of room temperature. Related rotated-Y cuts may be used if stability at another temperature is desired and the only changes required in design would be the use of different SAW velocities and electro-acoustic coupling constants.

Synthesis

Our initial approach for synthesizing the filter designs was to follow the work of Rosenberg and Coldren[1] in large measure because their technique accounted for losses. The approach developed by Matthaei[2], on the other hand, is a synthesis procedure which does not include losses (all unloaded resonance elements are assumed to have infinite Q values). Since the maximum unloaded Q's for our devices are given by Q_u = 10,500/F(GHz) (the maximum unloaded Q at 150 MHz is 70,000 for instance) we initially felt it necessary to use an approach which include losses. Three-pole (Type II) filters were designed (D271)[6], using Rosenberg's approach, with difficulty. Using his approach, however, we could not design a five-pole device. The reason for this difficulty was, as we found later, that it is necessary to properly set the cavity resonance frequencies (when the cavity is isolated) such that synchronous operation (all cavities resonant at the same frequency) is achieved when all cavities are coupled. The mathematical equations necessary to develop the cavity-frequency data may be in Rosenberg's[1] paper but this data is not readily extracted. Reluctantly, at first, we studied Matthaei's[2] synthesis techniques and very quickly found that these techniques were readily mastered and were surprisingly accurate in spite of the fact that acoustic losses are not considered. Further research showed us that the primary effect of losses is to cause a rounding of the filter passband response which effectively narrows the bandwidth. At lower frequencies, such as the VHF band, this rounding is not serious and to some extent can be compensated for by designing to a slightly wider bandwidth than is actually required. In actual practice a small amount of "tweeking" during analysis will yield the desired result.

Using Matthaei[2]'s approach we then developed a four-pole (Type II) filter (D279) and a six-pole (Type I) filter (D277). We now describe in

detail the synthesis and analysis procedures using these two designs as illustrative examples. The first issue in synthesis was to choose the basic filter configuration, that is, we had to decide which cavity-coupling techniques were to be used. Of the several techniques available[1] we considered transducer-coupling and reflector-coupling to be the only ones highly developed enough for our purposes. Also, used in well selected combinations, these two coupling schemes were all that we theoretically required to obtain the response desired. The combination of coupling schemes used effects the filter out-of-band rejection level, which we define as the difference between the passband and highest sidelobe level. To summarize a lot of work which we have done in this area, we have found theoretically that a minimum of two sets of transducer-coupled cavities are required to yield 60 dB of rejection. Reflector-coupling, though it is very economical space wise and it will allow shaping the filter response, does not yield high sidelobe rejection levels so this coupling scheme must be used with another. Thus a four-pole filter, which requires three cavity couplings, was designed to have two sets of transducer coupled cavities and one set of cavities coupled acoustically through a reflector. This is illustrated in Fig. 1 for the Type II - D279 design. The six-pole Type I filter, requiring five coupled cavity-pair, was designed to again have two transducer couplings and three reflector coupled pair as illustrated in Fig. 2. A three-pole filter was designed at first (D271) which simply had two transducer-coupled stages (three two-port resonators in cascade) but this proved to have a shape factor which was too large for the Type II requirements.

In order to use transducer-coupling, however, and theoretically make it unnecessary to use inductors between stages (capacitors, C_{ij}, are shown in Figs. 1 and 2), we have chosen to use the split-symmetric transducer configuration in each two-port single-pole resonant structure. The split-symmetric configuration, shown in detail in Fig. 3 as well as schematically in Fig. 1, allows longer transducers and hence higher cavity-coupling values than the conventional side-by-side transducers. This is so because the symmetric transducers select against the second order (antisymmetric) longitudinal cavity modes allowing longer cavities with more room for the transducers. Capacitors are shown in Figs. 1

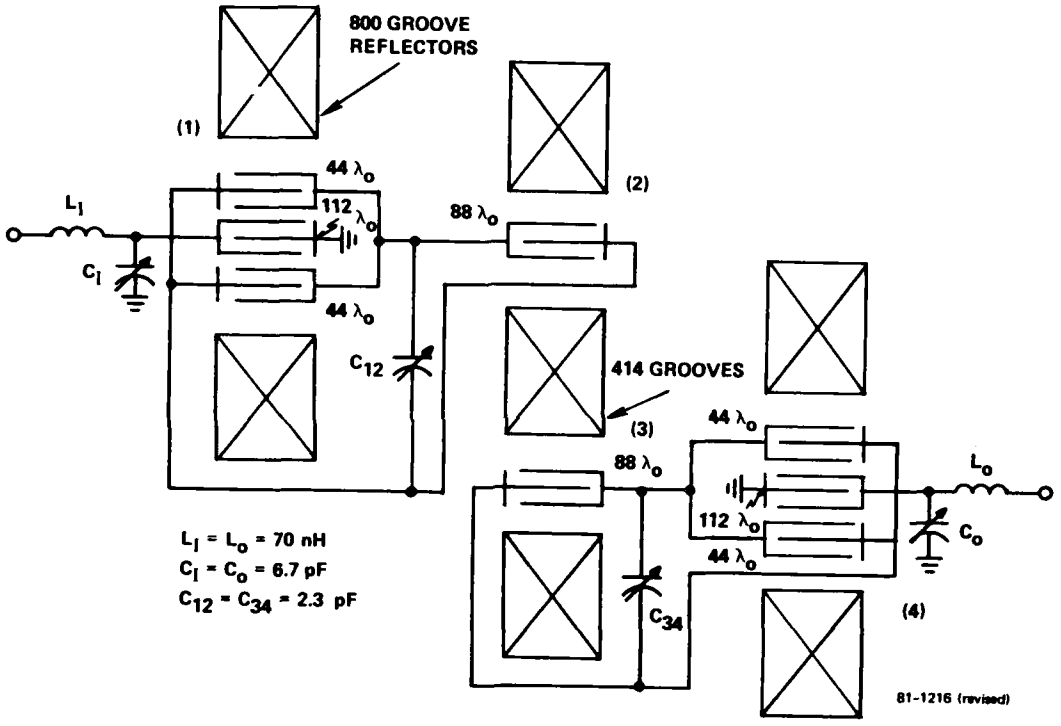

FIG. 1 Schematic of four-pole configuration with 2 transducer-coupled cavity-pairs and 1 pair coupled by a reflector. Component values shown are for the D279 filters.

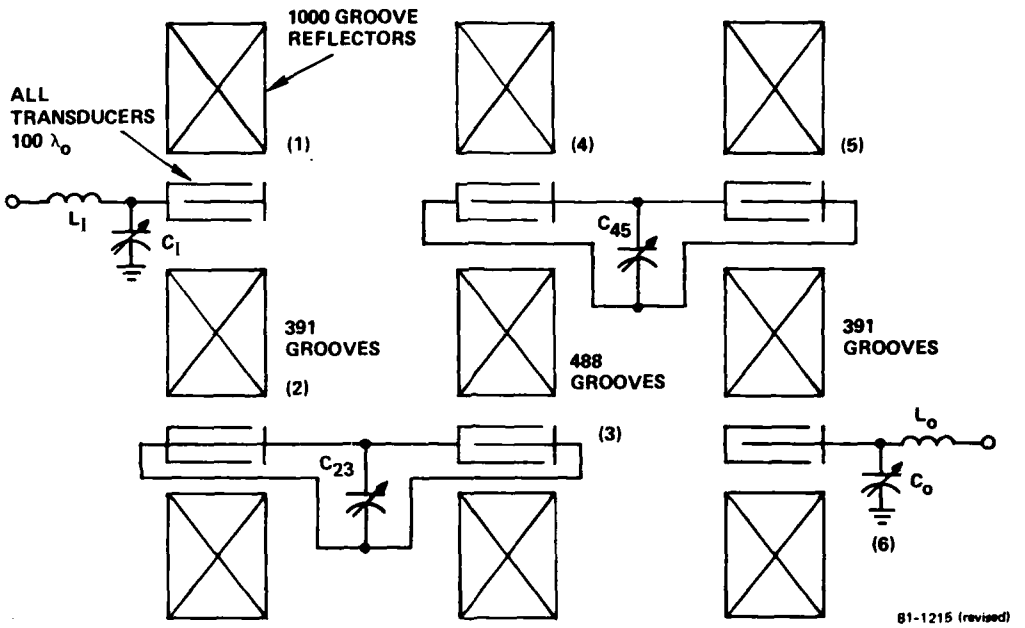

$L_I = L_o = 61$ nH $C_{23} = C_{45} = 8$ pF
$C_I = C_o = 4$ pF

FIG. 2 Schematic of six-pole configuration with 2 transducer-coupled and 3 acoustically coupled cavity pairs. Component values shown are for the D277 filters.

and 2 because we were unsure of the electro-acoustic coupling constant (k^2) value. We therefore designed longer transducers than necessary and could then decrease the cavity-coupling with a small variable capacitor mounted on the substrate.

The first step in synthesis was to select the groove-depth/metal-thickness and the reflector length (not the coupling reflectors which are sized later) for the system. The considerations here are: 1) to minimize the reflector length to keep the overall device size down especially in the VHF frequency range, and 2) to use as shallow a groove depth as possible to maximize the cavity Q and allow for a wider acoustic aperture. These are conflicting requirements which we resolved by calculating the cavity Q[7] for a range of depths and reflector lengths. For the four-pole Type II filter, for example, the data in Table II was calculated, for an assumed[7] $K_B = 10$, and a depth/length combination $h/\lambda = .012$ and 800 grooves was selected for use. A larger number of grooves required more space for a minimal increase in cavity Q, and increasing depth decreased the Q value rather quickly. Precisely

TABLE II

Cavity Q's (Units of 1000) for Various Depth (h/λ_o) and Reflector Lengths (Ng) for Type II Filters

depth/wavelength ratio h/λ_o	Number of reflector grooves (Ng)					
	700	800	900	1000	1100	1200
.006	22	32.2	42.5	51.4	58.1	62.6
.008	43.1	54.0	61.0	64.8	66.6	67.5
.010	53.0	63.4	65.6	66.5	66.8	66.9
.012	62.9	64.7	65.2	65.4	65.4	65.4
.014	63.0	63.5	63.6	63.6	63.7	63.7

how valid these results are is still open to question, however, it is the best we can do at present. For the Type I filters we chose $h/\lambda_o = .01$ and 800 grooves based on data similar to that in Table II.

We next had to select the acoustic aperture and in general we wish to have as wide an aperture as possible while minimizing the strength of the higher-order transverse-mode[8] responses. Work performed prior to this contract indicated that a 100 λ_0 (where λ_0 is the acoustic wavelength) aperture would be acceptable, but an initial experiment (D265) showed that the third order transverse made response was much too strong. Thus we chose an aperture of 48 λ_0 for D277 and D279 but we have further reduced this to 40 λ_0 for designs afterwards.

The material parameters such as velocity, capacitance, and electro-acoustic coupling constant (k^2) had to be ascertained for use in the synthesis routine. We had previously done experimental work to determine the velocity in the reflectors as a function of groove depth[3] and in the recessed transducer[8]. The free surface velocity was also found[3] to agree with calculation at a value of 3157.6 ± 0.2 m/sec. These velocities are required in the analysis routines to establish the period for the transducers and reflectors, and the gaps in the cavities in order to attain the desired resonance frequencies. In spite of this effort we still found it necessary to trim[10] the cavity frequencies following device fabrication. The capacitance per meter on ST quartz for quarter-wave electrodes on half-wavelength centers is well established to C_1 = 25.2 pF/m. An accurate value of k^2 was more difficult to establish since there is some disagreement in the literature[11], and we had no firm experimental results to work with. For the initial designs (D277 and D279) we used k^2 = .0016 which is based on experimental data[11]. However, we believe that this value is too high since we could not get good agreement between theory and experiment for the D277 and D279 devices. The coupling capacitor values, C_{ij} in Figs. 1 and 2, required by experiment to yield an acceptable passband response did not correspond to the values shown on the figures. Due to difficulties in fabrication and measurement we cannot state what the required coupling component values were, indeed, in several instances an inductor (L ~ 1 μh) seemed to yield the best result. Comparison of experimental work, provided to us by Rosenberg[12], with analyses performed here at Sperry Research on two-pole transducer-coupled filters indicates that the k^2 = .0011 is more nearly correct. We plan to use this value for future designs while carefully monitoring the results.

The transducers were all overlap-weighted using the cosine function in order to suppress the 3rd and higher order transverse mode responses. This function seems to perform as well as more accurate ones described in the literature[13] and the actual split-symmetric transducer version is seen in Fig. 3. For a single transducer in a cavity such as we see in the reflector-coupled cavities of Fig. 1 and 2 the symmetric transducer is made to have the center electrode on the centerline of the cavity. Overlap weighting causes two problems in analysis, however. The first is the uncertainty as to how well the transducer shape conforms to the acoustic mode shape and this is reflected as an uncertainty in k^2. The second problem is that the model used in analysis assumes an unweighted transducer (with a sin x/x filter response) and the actual device filter response, upon which the resonance response is superimposed, is something different. This is shown in Fig. 4 where the experimental response of two cosine-weighted transducers, transmitting through a reflector is given. The result of this difference is primarily an inaccuracy in the prediction of the rejection level. Our model can be updated to include the weighted transducer and we shall perform this is the next phase of the program.

The free-surface gap lengths within the resonant cavities should be kept as small as possible in order to allow for the longest possible transducer. The fabrication procedures, however, require that the gaps between transducer and reflectors be at least several wavelengths. Also, for two-port cavities we wish to have enough separation between transducers to reduce direct electromagnetic feedthrough to acceptable levels. This feedthrough is due to inter-transducer capacitance. We have chosen to use 3 λ_0 as the gap length between transducers and reflectors and between transducers in D279, and 6 λ_0 in D277 and this length appears to be adequate for both fabrication and feedthrough suppression. Having established the basic configuration and several of the design parameters (aperture, outside reflector length, k^2, capacitance, etch depth, gaps, etc.) the remaining parameters (transducer lengths, coupling reflector lengths, and matching component values) are determined using the synthesis procedure[2]. We now show how we have synthesized the two designs (D279 and D277) for the devices delivered in Phase I of this program. For a more complete understanding of the procedure we refer the reader to Ref. 2.

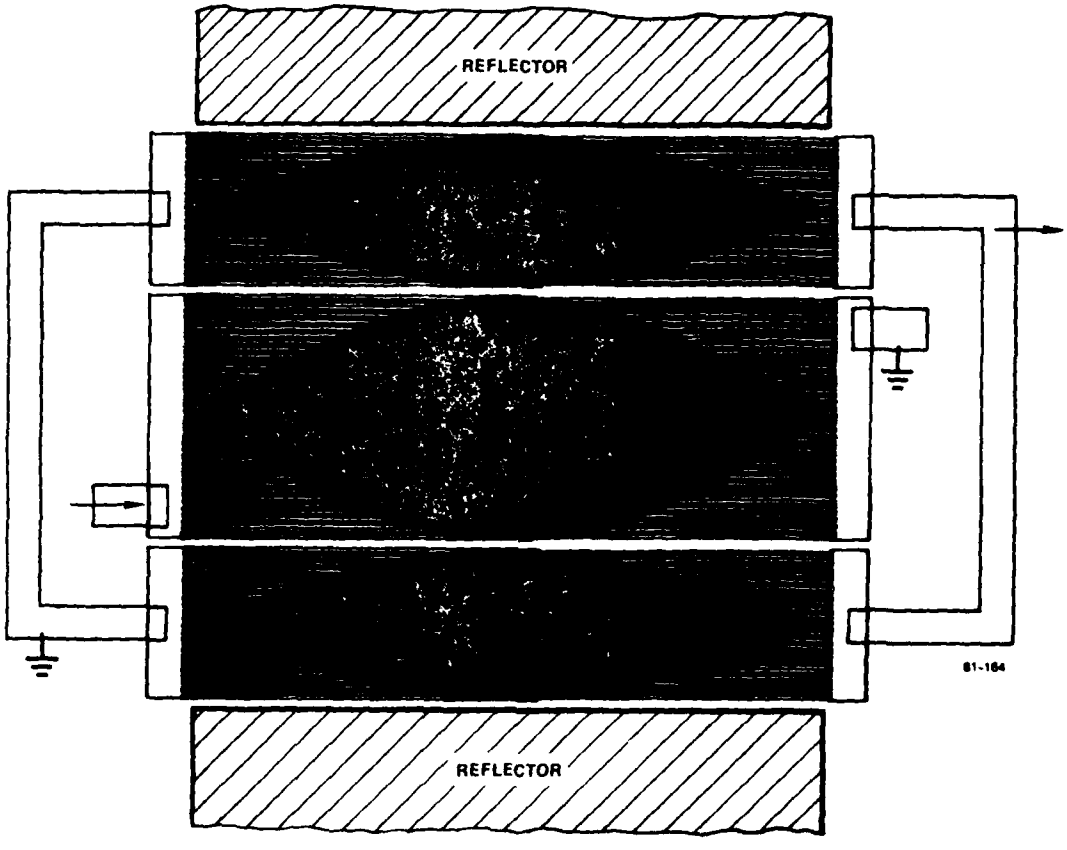

FIG. 3 Split-symmetric cosine weighted transducer configuration in a two-port resonator cavity.

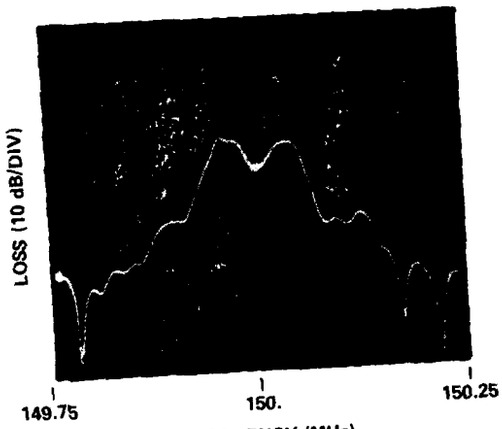

(a) FREQUENCY RESPONSE

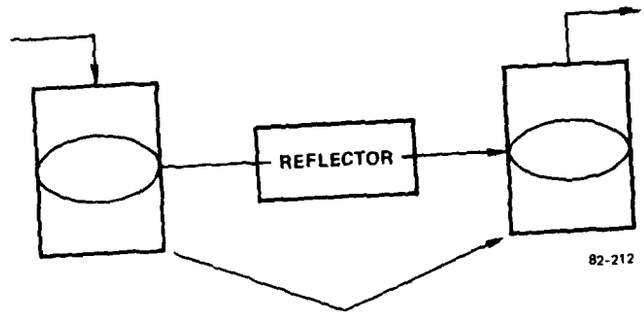

COSINE WEIGHTED TRANSDUCERS

(b) CONFIGURATION

FIG. 4 Frequency response (section a) of two cosine-weighted transducer with a reflector in the acoustic path.

For D279, which we desired to meet the Type II filter specifications of Table I, we decided to use the four-pole scheme of Fig. 1. We had to initially select transducer sizes, then synthesize the coupling reflector length and matching component values, analyze the design and iterate if required. As it turns out, iteration was required because we wished to have the coupling components between transducers to be capacitors (C_{12} and C_{34}) and the rejection level decreased to unacceptable levels for certain combinations of transducer lengths. The procedure begins by selecting the "low-pass prototype" element values (g_i's) tabulated in Ref. 14 for various filter types. For the four-pole 0.5 dB ripple Chebychev (Type II) filter Table 4.05-2(a) of Ref. 14 yields the element values in Table III.

Table III

Lowpass Prototype Element Values for the Type II Filter

g_0	g_1	g_2	g_3	g_4	g_5
1.0	1.6703	1.1926	2.3661	0.8419	1.9841

The inverse filter Q, designated[2] as W, is given by (1).

$$W = \frac{\Delta F_3}{F_0} \qquad \frac{1}{Q_F} \tag{1}$$

where ΔF_3 is the filter bandwidth between the 3 dB points, F_0 is the center frequency, and Q_F is the filter Q. The input/output electrical Q values Q_{E1} and Q_{E5} are defined by (2):

$$Q_{E1} = \frac{g_0\ g_1}{W} \quad ; \quad Q_{E5} = \frac{g_4\ g_5}{W} \tag{2}$$

and the intercavity coupling constants $k_{j,j+1}$ are computed from (3).

$$k_{j,j+1} = \frac{W}{\sqrt{g_j\ g_{j+1}}} \tag{3}$$

The above expressions for Q_{Ej} and $k_{j,j+1}$ are from Table I Ref. 2 with W'_1 (of Ref. 2) set to unity. The expressions required to calculate other quantities are summarized below:

b_j - susceptance slope parameter for cavity j

$$b_j = b_{j-1,j} + \frac{M_j \pi}{2} + b_{j,j+1} \tag{4}$$

where M_j is the edge-to-edge cavity length in half-wavelengths, and $b_{j,k}$ is the slope parameter associated with a reflector array on one side of the cavity. The quantity $b_{j,k}$ is calculated using Eq. 8 of Ref. 2 for each reflector using design value of groove number and etch depth (where $u = \varepsilon = 1 + 1/2 \ \ h/\lambda_o$ for grooves[3]).

$J_{j,j+1}$ - impedance inverter between cavities

$$J_{j,j+1} = k_{j,j+1} \sqrt{b_j \, b_{j+1}} \tag{5}$$

and for coupling reflector ($N_{j,j+1}$ grooves)

$$J_{j,j+1} = \left(\frac{1}{U}\right)^{N_{j,j+1}} \tag{6}$$

Equation (5) above applies to any form of coupling (transducer and reflector) and we see that for reflectors we have two constraints determining the reflector length. In the design procedure we must therefore iterate, first selecting a coupling-reflector length (Ng) calculating J from (6) and comparing it with the J value from (5), which is itself a function of Ng. Fortunately, the J value from (5) is a slowly varying function of Ng (through the b_j value) and only one iteration is usually required. Since the procedure for synthesis is slightly intricate and somewhat confusing, we now simply tabulate various parameters used, to illustrate the technique.

Table IV

Type II Filter Parameter Values in Synthesis

N_p	88	112	(No. of transducer wavelengths.)
C_T	2.8428 pF	3.6182 pF	(total transducer capacitance x $2/\pi$ to account for cosine weighting)
$4/\pi\ k^2\ N_p$	.1793	.2281	
G_o	4.804×10^{-4}	7.778×10^{-4}	$G_o = 4/\pi\ k^2\ N_p \omega_o C_T$ (ω_o = radian frequency = $2\pi F_o$)
J_T	.03099	.03944	$\sqrt{2G_o}$ - transducer impedance inverter parameter
G_j		.1372	$G_j = g_j/Q_{Ej}$ (input/output transducer admittance-before inversion)
G_{xj}		.01134	J_T^2/G_L (inverted transducer admittance)
R_{pj}		88.202	$R_{pj} = 1/G_{xj}$ (transducer parallel resistance)

The parameters G_j, G_{xj}, and R_{pj} are calculated only for the input/output transducers, which referring to Fig. 1 have N_p = 112 wavelengths.

Table V

Type II Filter Additional Parameter Values

(Ng = 414, h/λ_o = .012)

	j	g_j		k_{ij}		$J_{j,j+1}$	b_j		$\Delta M_{cj}(\lambda_o)$
input	0	1							
cavity numbers	1	1.607					927.8		
			12	1.748×10^{-4}	12	.12756		12	.02030
	2	1.1920					574		
			23	1.4688×10^{-4}	23	.08431			
	3	2.3661					574		
			34	1.7477×10^{-4}	34	.12754		34	.02030
	4	.8419					9278		
output	5	1.98411							

The parameter ΔM_{cj}, given by (7), is the cavity length correction required to compensate for loading effects of one cavity on another.

$$\Delta M_{cj} = = \frac{\left|J_{j,j+1}\right|}{\pi} \quad \frac{\lambda_o}{2} \tag{7}$$

For D279, this correction is applied to cavities 2 and 3 only since the input/output impedance matching networks of Fig. 1 perform this compensation for cavities 1 and 2. The value ΔM_{cj} is equivalent to a shift in resonance frequency downward since the cavity is being made longer, and here we see how simply Matthaei's approach yields this data. We now illustrate the procedure used to find Ng for the coupling reflector between cavities 2 and 3 (see Fig. 1). Cavities 1 and 4 are $212\lambda_o$ long (total transducer lengths = 200 λ_o plus four 3 λ_o gaps) and the reflectors have 800 grooves .012 λ_o deep. Thus the slope parameter for cavities 1 and 4 are

$$b_1 = b_4 = 130.88 + \frac{424\pi}{2} + 130.88 = 927.8$$

For cavities 2 and 3 we have an 88 λ_o transducer plus two 6 λ_o gaps for a cavity length of 100 λ_o. Thus the slope parameter for each is

$$b_2 = b_3 = 130.88 + \frac{200\lambda}{2} + x$$

where x is the slope parameter of the coupling reflector which we have yet to specify in length. Choosing Ng = 400 we find that x = 128.7 and $b_2 = b_3 = 573.74$. From (6), $J_{23} = .0914$ requiring that $b_2 = b_3 = 622.3$ which is larger than the value of 573.74. We have produced a Table of values for $J_{j,j+1}$ and $b_{j,j+1}$ for various reflector lengths (Ng) and etch depth (h/λ_o), which is reproduced as Appendix I. From this Table for r = 1.006 (h/λ_o = .012) we find that $b_{j,j+1}$ varies very slowly while $J_{j,j+1}$ changes much more quickly. By increasing the value of Ng from 400 to 414, we change b_{23} from 128.71 to 129.04 and J_{23} goes down to .08401. The new value of $b_2 = b_3 = 573.82$ (very little change) while J_{23} from (5) is now .08428 which is close enough to .08401

(for Ng = 414) to be acceptable. Thus we see that only one iteration was necessary to find the $J_{j,j+1}$ values given in Table V.

The reflectors, transducers, and cavity length corrections have now been found for D279 and we must next determine the coupling capacitor value (C_{ij}) and the input/output matching circuit values. The first point to note here is that even though the values of g_j in Table V are nonsymmetric, the coupling values (J) and cavity corrections (ΔM) are very nearly symmetric and for all practical purposes we have a symmetric system. Thus, referring to Fig. 1, L_I, C_I and C_{12} are equal to L_o, C_o and C_{34} respectively. The coupling capacitor (more properly a decoupling capacitor since it functions to decrease the inter-cavity transfer of energy) value is readily found from (8)

$$C_{j,j+1} = 2\, C_T \left[\frac{4k^2\, N_p}{\pi\, J_{j,j+1}} - 1 \right] \tag{8}$$

Thus utilizing the values for C_T and $J_{j,j+1}$ in Tables IV and V, we find that the required value of $C_{12} = C_{34} = 2.3$ pF. The input/output matching circuit values may be found, with reference to Fig. 5, using the following procedure: (a) Calculate a value of C_p which, in parallel with C_T, will reduce the R_p to R_g when the parallel combination (C_p + C_T + R_p) is changed to the equivalent series capacitance-resistance combination, (b) calculate a value of L which neutralizes the series equivalent capacitance found in (a). A simple sequence of formulae used to perform the above step is given below and the "cook-book"

$$X_T = \frac{1}{\omega_o\, C_T} \tag{9}$$

$$R_S = \frac{R_p\, X_T^2}{R_p^2 + X_T^2} \tag{10}$$

$$X_C = \frac{R_S}{\sqrt{\frac{R_S}{R_g} - 1}} = \frac{1}{\omega_o\, (C_T + C_p)} \tag{11a}$$

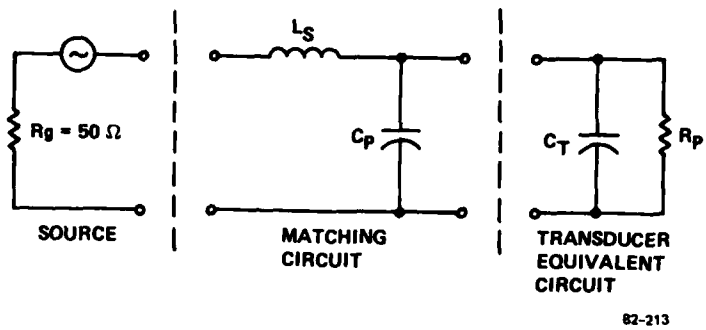

FIG. 5 Schematic diagram required to understand the matching circuit.

$$C_p = \frac{1}{\omega_o X_c} - C_T \qquad (11b)$$

$$X_S = \frac{X_c R_p^2}{R_p^2 + X_c^2} = \omega_o L_s \qquad (12)$$

procedure is to use the values of C_T, R_p and ω_o found earlier to calculate to C_p from (11b) and L_s from (12). This procedure is straightforward and accurate and the numbers are given in Table VI below for D279:

Table VI

Matching Circuit Values Calculated for D279

$\omega_o = 2\pi\ 150 \times 10^6$	$X_T = 293.25$
$C_T = 3.618$ pF	$R_S = 80.88$
$R_p = 88.2$ pF	$X_p = 102.92$
	$C_p = 6.7$ pF
	$X_s = 43.58$
	$L_s = 46.24$ nh

This completes our descripton of the synthesis procedure and the illustration of this technique for D279 (Fig. 1)

We now summarize this for D277 (the six-pole Type I filter) which was fabricated and delivered to NRL. Performing an analysis, similar to that which resulted in Table II for D279, we found that a relative groove depth (h/λ_o) of .01 and outside reflectors with 1000 grooves yielded the optimum cavity Q value. Since the Type I filter resonance frequency is 217 MHz and the wavelength is commensurately shorter than the 150 MHz Type II design, the 1000 groove reflector yields a device which is well within overall length constraints. For this etch-depth the velocities[3,9] in both the reflectors and recessed transducers is about 3154 m/sec and this is the value used in the analysis to establish the wavelength. The configuration of Fig. 2 was selected as being most

economical in space and yielding an acceptable (theoretically) level of rejection. As for D279, we used an aperture of $48\lambda_o$ and cosine-weighted symmetrically located transducers. For the six-pole Butterworth response (Type I) filters, Table 4.05-1(a) of Ref. 14 gives the required low-pass prototype element values listed below in Table VII. We note first of all that the values of g_j are symmetric and this results from the fact that the filter is a lossless-Butterworth design. We compare this symmetry with the asymmetry of the even-order Chebychev design (for example, D279). Odd-order lossless Chebychev designs are exactly symmetric. When losses are included, all designs become asymmetric[1].

Table VII

Type I Filter - Design Parameter Values for Synthesis

	j	g_j		k_{ij}	$J_{j,j+1}$		b_j	$\Delta M_{cj}(\lambda_o)$
input	0	1.0			01	.4854		
	1	.5176	12	2.154×10^{-4}	12	.1422	660.17	
	2	1.414	23	1.115×10^{-4}	23	.0736	660.17	.0177
cavity	3	1.932	34	1.326×10^{-4}	34	.0876	663.57	.014
number	4	1.932	45	1.115×10^{-4}	45	.0736	663.57	.014
	5	1.414	56	2.154×10^{-4}	56	.1422	660.17	.0117
	6	.5176			67	.4854	660.17	
output	7	1.0						

N_p	C_T	$4/\pi k^2 N_p$	G_o	J_T	G_j	G_{xj}	R_{pj}
100	2.235	.20375	6.207×10^4	.03524	.2351	.00528	189

In this design we chose to make all transducers equal in length (N_p = 100 in Table VII), with $3\lambda_o$ gaps, since adjustments in coupling could be effected by varying the length of the coupling reflectors and the matching/coupling component values. We believed that N_p = 100 would result in (de)-coupling capacitor (C_{23} and C_{45} of Fig. 2) values which were manageable, that is, not being too small and subject to being

overpowered by parasitic capacitances. Since the value of $k^2 = .0016$ chosen was larger than we now believe to be correct, the 100 λ_o transducers did not yield good results when (de)-coupling capacitors were actually used. The calculations required to find the coupling reflector lengths, input/output matching circuit values, and coupling capacitor value were then found as described earlier for D279 and these values are shown in Fig. 2.

Analysis

Following synthesis, we analyzed each design to see how well the synthesis procedure worked. We found that the procedure worked very well, and that only a few minor adjustments (coupling or matching component values) were required to achieve a computed response which we considered satisfactory. Perfection was, in general, not possible due to the losses included in our analysis and the large number of parameters which could be in error and adjusted. From the analysis, we also determined the exact frequencies to which each cavity (when isolated) must be set to achieve the response desired, and the required transmission response of each reflector-coupled cavity-pair. During fabrication we then knew where to set the cavity frequencies and how to adjust coupling-reflector coupling strength.

We had a number of computer routines, developed for internal use though during our previous work with resonators, which allowed us to analyze resonators with various combination of reflectors and transducers. The routines utilize the Mason equivalent circuit model[15] (cross-field) with viscous, air, and bulk mode losses, and electrical feedthrough included. The calculations for an N element reflector or transducer are made in closed form using the matrix techniques developed by Field, Ho and Chen[16]. In this technique, we calculate the appropriate matrix elements for a single "cell", consisting of a complete reflector or transducer segment, and then raising this matrix to the Nth power we obtain the matrix for an N element array. This makes N matrix-multiplications unnecessary and reduces the computation time by orders of magnitude since N can be as high as a thousand. The single limitaton on this technique is that one cannot model weighted transducers or reflectors. We must revert to previously developed routines, which

take much more computer time, to model weighted structures. In the model, we can also vary the velocity directly or by adding reactances[17] at the element edges.

In order to model the structures used in this program, we first had to develop a routine to analyze the split-symmetric transducer two-port resonator of Fig. 3. We then had to develop routines which would allow us to cascade various acoustic strutures such as we show in Figs. 1 and 2 with variable matching/coupling networks. The scheme which we adopted is illustrated in Fig. 6. For each of M frequencies the ABCD matrix is computed and stored for an acoustic structure (two-port single-pole resonators, or two-pole acoustically-coupled resonator). The coupling/matching network configuration is then defined and the ABCD matrix for the entire structure is computed. From this complete ABCD matrix, all the interesting electrical parameters of the filter are determined and plotted. Since recomputing the complete matrix is very rapid when only the coupling networks are changed, this procedure is extremely efficient and allows us to analyze and tweek the various configurations in a short period of time.

We now present the results of calculations for D279 followed by similar results for D277. In Figs. 7, 8, and 9 we show the filter response, for varying bandwidths, for the structure of Fig. 1. These results are computed for a device with no air loading since the device will ultimately be sealed in a vacuum. We note the salient features of the computed response and compare these with the specifications (of Table I) in Table VIII. First of all, we did not achieve the Chebychev bandpass (with three dips for a four-pole). A review of the literature indicates that it is frequently very difficult to achieve the theoretical passband response and our experience bears this out. Rather than spend a lot of

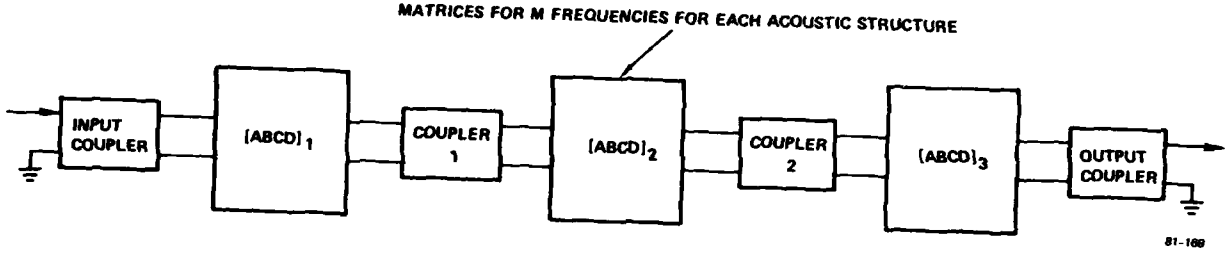

FIG. 6 Schematic representation of our scheme for efficient computation of the response of a multipole filter. Coupler matrices are recomputed as these components are varied for each of the M frequencies.

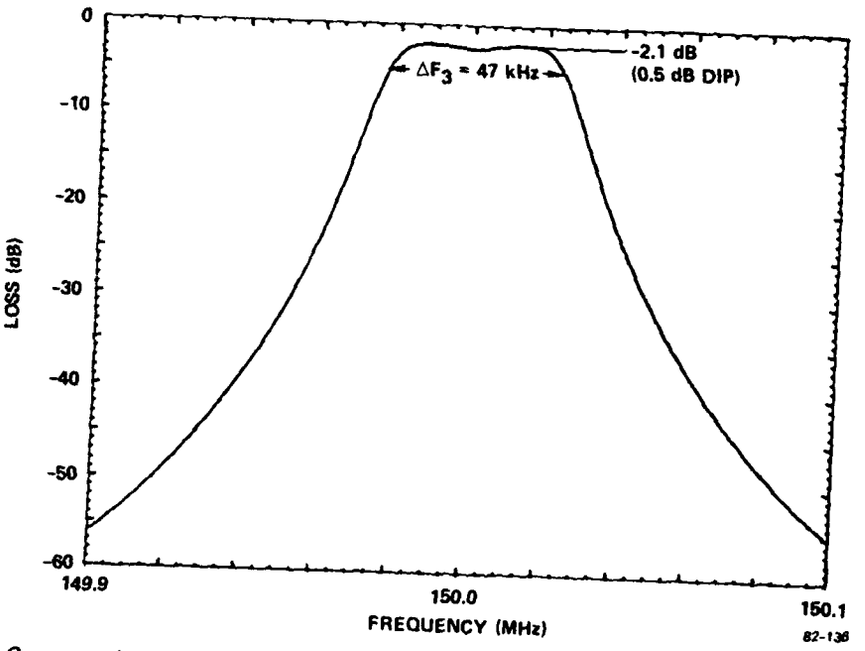

FIG. 7 Computed narrowband response for D279 with component values as given on Fig. 1.

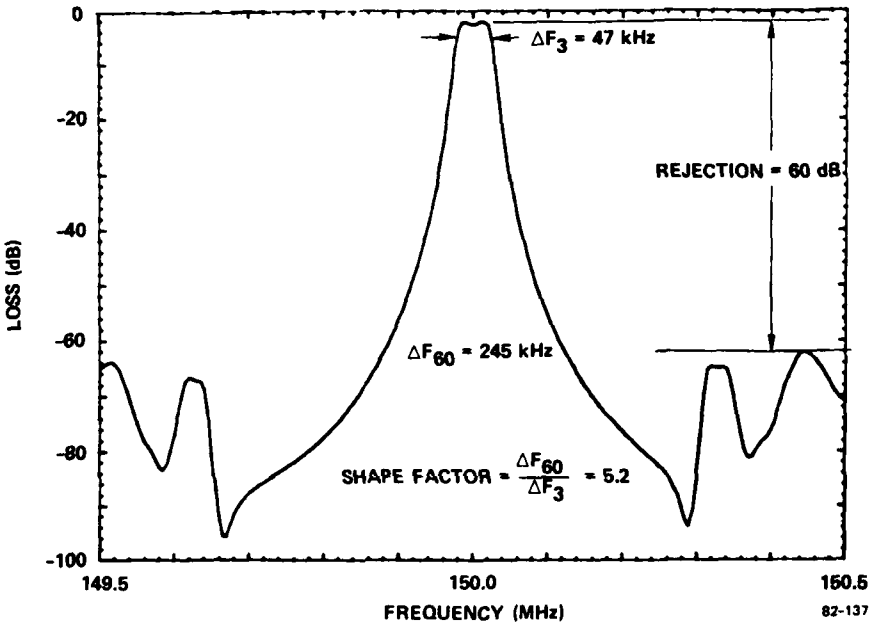

FIG. 8 Computed response for D279 with component values as given on Fig. 1.

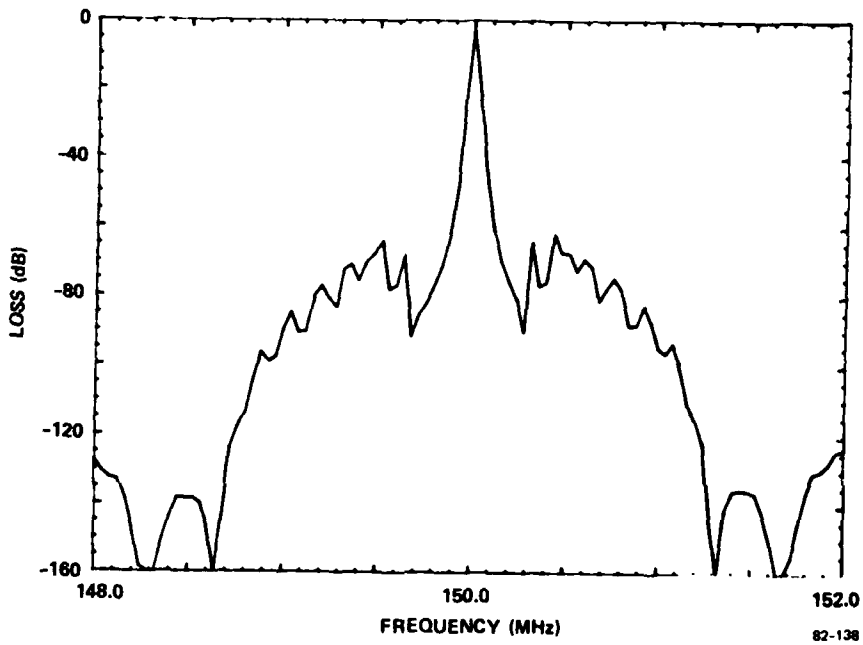

FIG. 9 Computed wideband response for D279 with component values as given on Fig. 1. Note that, the acoustic response is down 110 dB at $F_O \pm 1.1$ MHz.

Table VIII

Desired and Predicted Response for D279

	Desired	Predicted
Loss	6 dB max	2.1 dB
ΔF_3	37 kHz min	47 kHz
Shape Factor (60/3dB)	8.1	5.2
Response Shape	Chebychev (3 dips - 0.5dB)	Single Dip (0.5dB)
Minimum Rejection at		
$F_R \pm 0.15$ MHz	60 dB	66 dB
$F_R \pm 0.5$ MHz	80 dB	60 dB
$F_R \pm 5.0$ MHz	110 dB	135 dB

time tweeking the design to produce the 3-dip response we accepted the response of Fig. 7. Secondly, we see that the 3 dB bandwidth is wider than required and that the shape factor is smaller than specified, both characteristics being favorable. The predicted loss of 2.1 dB is well under required 6 dB, leaving significant room for unaccounted for losses and errors. Since the shape factor was low (which is good) it is no surprise the find that the rejection at $F_0 \pm 0.15$ MHz exceeds the required 60 dB. However, at 0.5 MHz effect the rejection is much poorer than desired (60 vs. 80 dB) due partly to the reflector-sidelobe ripple but more importantly to the basic non-resonant response of the transducers. Further, this non-resonant response of Figs. 8 and 9 is in error since the transducers are not apodized in the model but they are in the device. We shall see in the presentation of the experimental results that we indeed did not achieve the desired rejection level and these computer results show that a re-evaluation of the configuration, or a substantial redesign of the exiting configuration is necessary.

Further computed results are shown in Fig. 10 where the VSWR (of the passband) is given, and in Fig. 11 where the Smith chart plot of the input (and output since they are the same) impedance is shown. Further

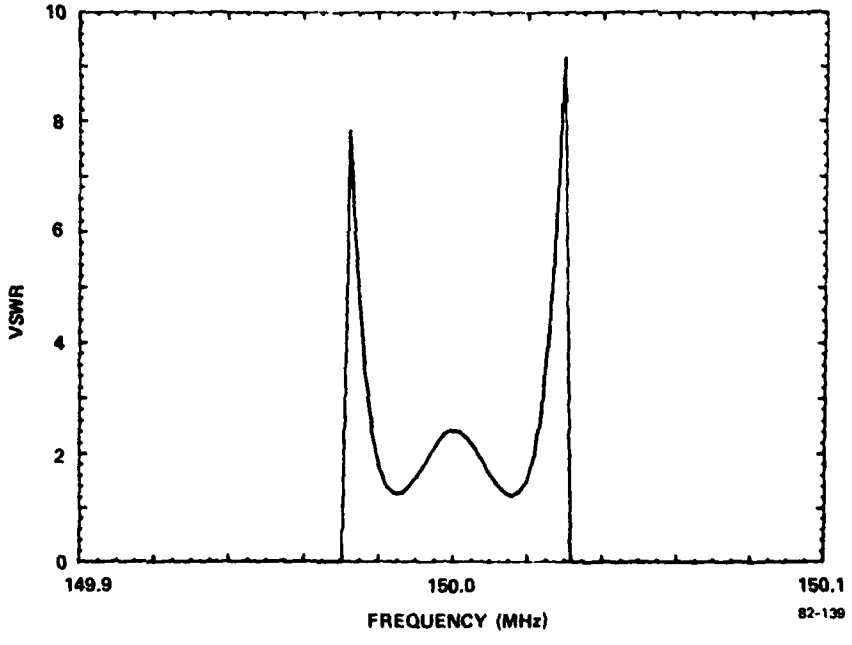

FIG. 10 Voltage standing wave ratio (VSWR) for D279.

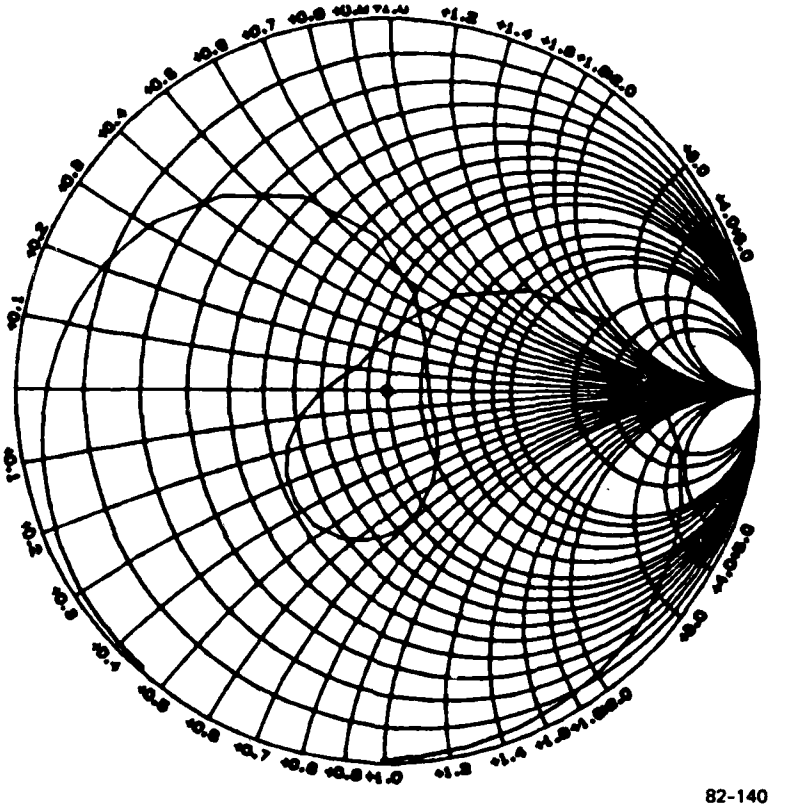

82-140

FIG. 11 Smith chart plot of the input (and output) impedances for D279 as shown on Fig. 1. The total bandwidth is 200 kHz as on Figs. 7 and 10.

improvement (increased linearity in VSWR) in those characteristics can only be achieved by modifying the passband response. In Fig. 12 we show the response of the acoustically-coupled pair (two-pole) consisting of cavities 2 and 3 of Fig. 1. When fabricating the device we endeavor to replicate this response experimentally by first setting the cavity frequencies and then the coupling strength (through the reflector) using our frequency-trimming and coupler-trimming techniques. In Fig. 13 we show the computed electrical reflection coefficient magnitude, $/\Gamma/$, for cavities No. 2 (or 3 as they are the same in all respects for D279) with the transducer in the opposite cavity open circuited, electrically unloading that cavity. The reason for computing $/\Gamma/$ (and measuring it) in this manner is that we obtain a dominant resonance (seen at the lower frequency ~ 149.96 MHz of Fig. 13) which we can conveniently measure and adjust. When both cavities of an acoutically-coupled pair are not on the same frequency, which is generally the case as fabricated, it is very difficult, if not impossible, to adjust each frequency correctly with the other cavity loaded due to the coupling effects. In Fig. 14 we show the computed response for the two-port cavities (1) or (4) for D279. From this curve we find the resonance frequency to which these cavities must be trimmed in order to obtain the response of Fig. 7. The calculations for Figs. 12 through 14 were performed with air-losses included because the required measurements during fabrication are most conveniently done in air.

The question of how accurately we must set the cavity frequencies naturally arises and we have performed calculations showing that frequency errors on the order of 10 percent of the filter bandwidth have no appreciable effect on the filter response. For D279 this acceptable error is about 4 kHz, and we are experimentaly able to meet this requirement with no difficulty. The important measure of the error is its fraction of the center frequency (F_R). For example, 4 kHz at 150 MHz is about 25 parts-per-million (ppm) and we can readily trim to less than 10 ppm. Thus, narrow filter bandwidths or high frequency (> 600 MHz) could be significantly more difficult to make than the Type I and II filters in this program.

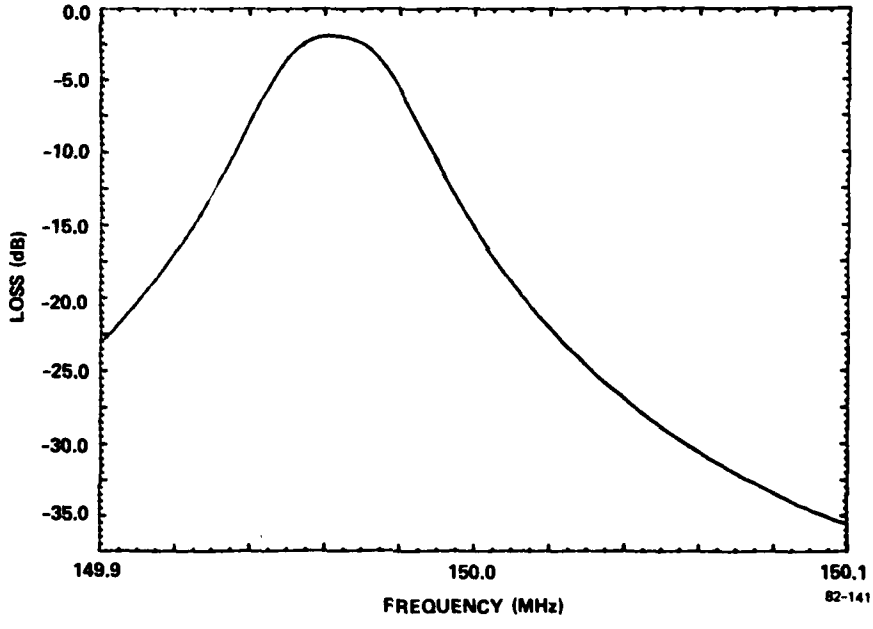

FIG. 12 Computed response of the acoustically-coupled cavity-pair for D279 (central section of Fig. 1) unmatched.

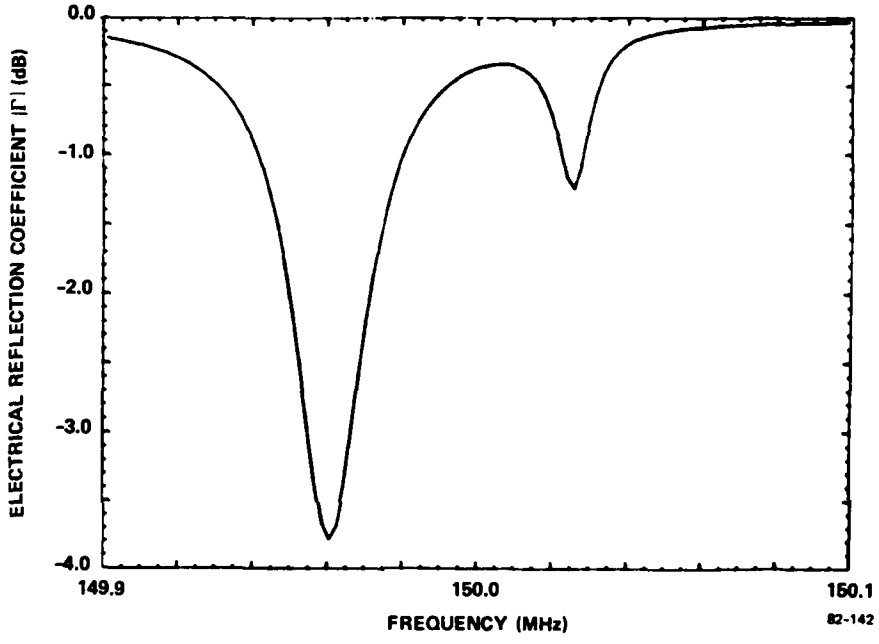

FIG. 13 Computed reflection coefficient magnitude, $|\Gamma|$, for cavity No. 2 of D279 (central section of Fig. 1) of the acoustically coupled pair with cavity No. 3 electrically unloaded.

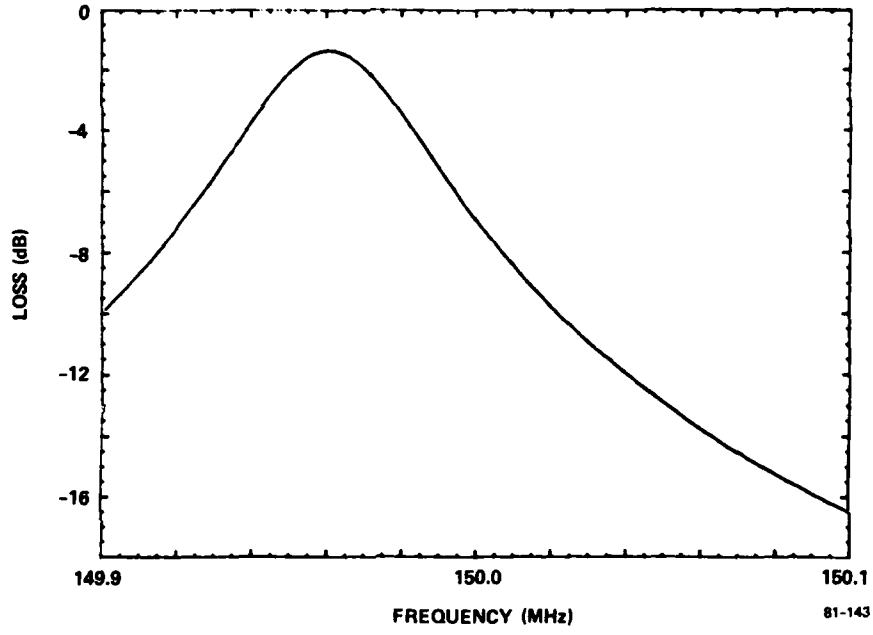

FIG. 14 Computed response for one of the two-port resonators of D279 (Fig. 1) unmatched into 50 Ω.

For the D277 filter Figs. 15 through 24 show all the computed data necessary to assess the design and fabricate the devices. The salient aspects of the response are compared with the specifications in Table IX. We see that the design response exceeds all requirements by a significant

Table IX

Desired and Predicted Response for D277

	Desired	Predicted
Loss	10 dB max	4.3 dB
ΔF_3	40 kHz	48 kHz
Shape Factor (60/3 dB)	4	3.5
Response Shape	Butterworth	Butterworth
Rejection outside:		
$F_R \pm 1$ MHz	60 dB	74 dB
$F_R \pm 2$ MHz		140 dB

amount which increases the probability of fabricating devices which meet specifications. The data of Figs. 15 through 19 is self explanatory and shall not be discussed further. The response of Fig. 20 is of interest since it shows the transmission response which we must have for cavities No. 1 and 2 (or No. 5 and 6) of Fig. 2. Both of these cavities are to be trimmed to different frequencies as shown on Figs. 21 and 22 where the cavity resonances for $|\Gamma|$ are shown. We note that Fig. 20 has a large dip in the passband, which is due both to a high level of coupling and to the differing cavity resonance frequencies. For cavities No. 3 and 4, the resonance frequencies are to be the same (due to symmetry in the structure) at a value found on Fig. 24, and the transmission response is as seen on Fig. 23. The response of Fig. 23 shows an almost critically coupled cavity-pair response which we must replicate experimentally. As with D279, all responses are calculated with air losses included except the overall filter response, Figs. 15-19.

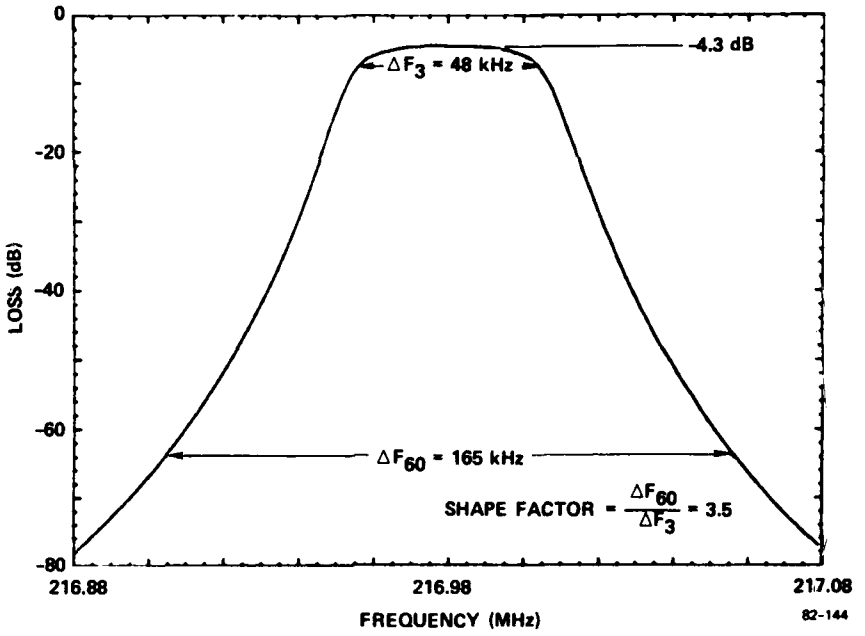

FIG. 15 Computed narrowband response for D277 with component values as given on Fig. 2.

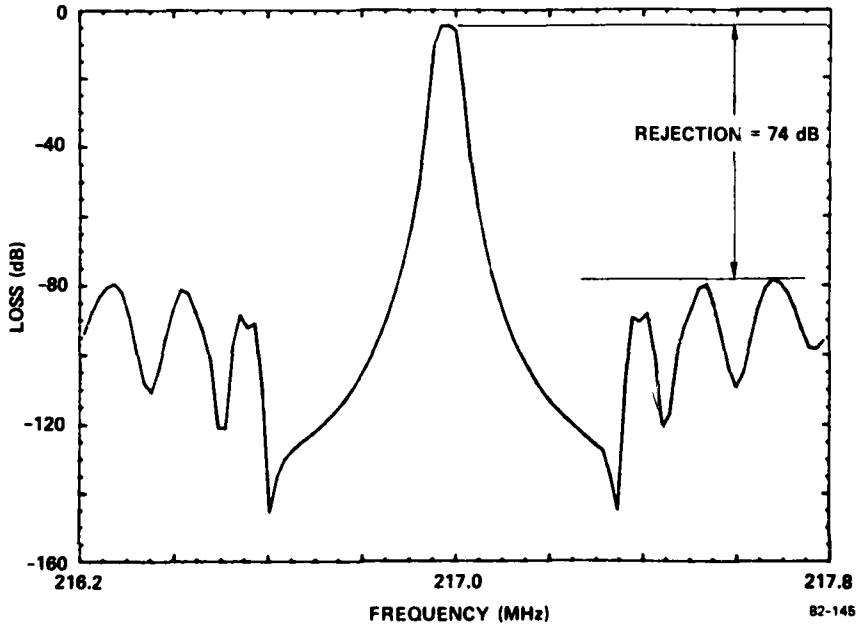

FIG. 16 Computed response for D277 with component values as shown on Fig. 2.

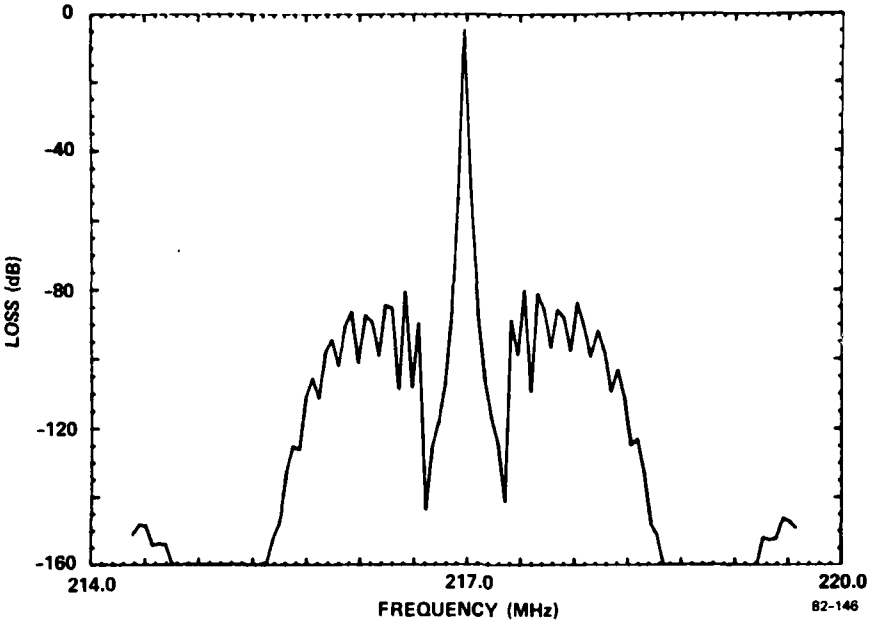

FIG. 17 Computed wideband response for D277 with component values as shown on Fig. 2.

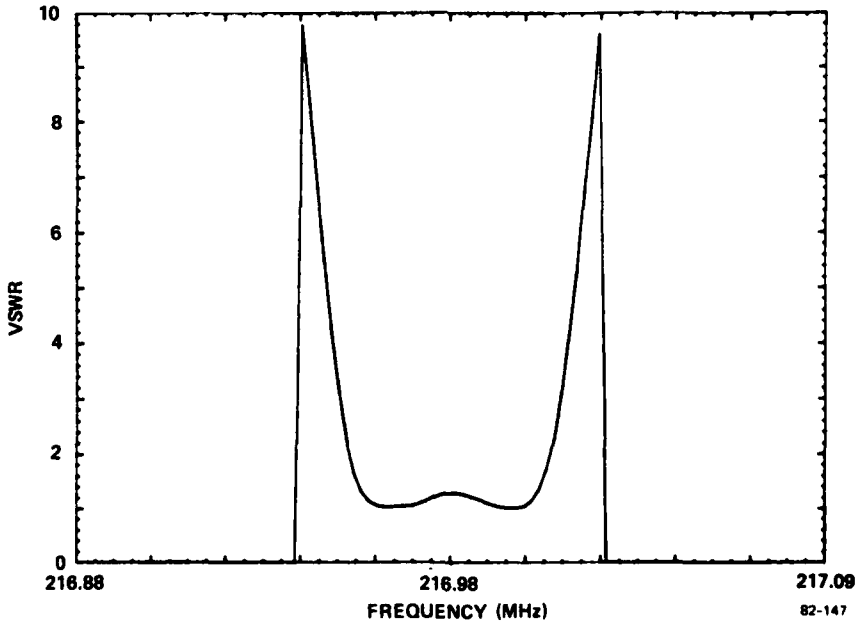

FIG. 18 Voltage standing wave ratio (VSWR) for D277.

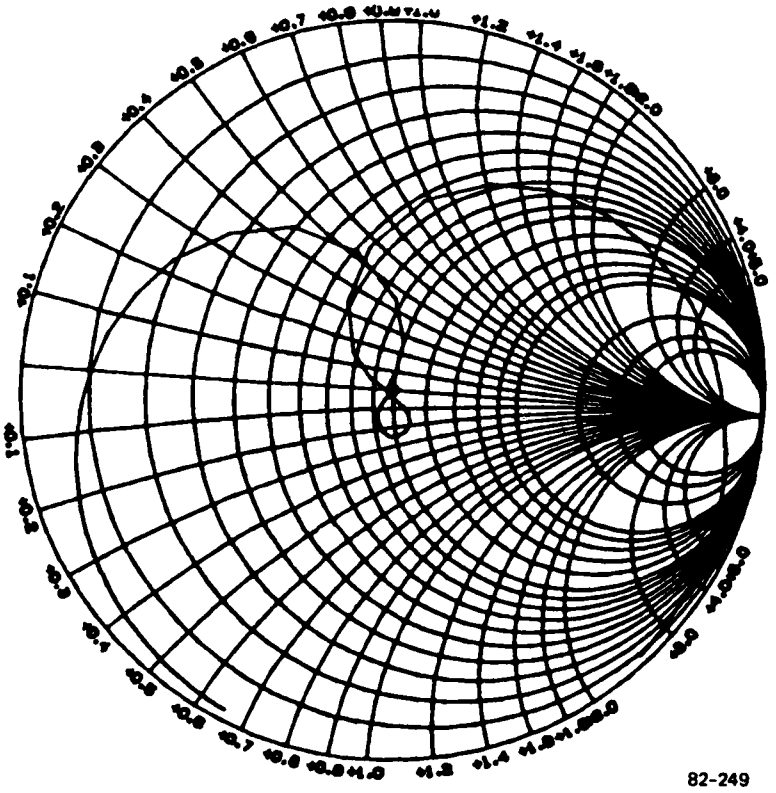

82-249

FIG. 19 Smith chart plot of the input (and output) impedances for D277, as shown on Fig. 2. The total bandwidth is 200 kHz as on Figs. 15 and 18.

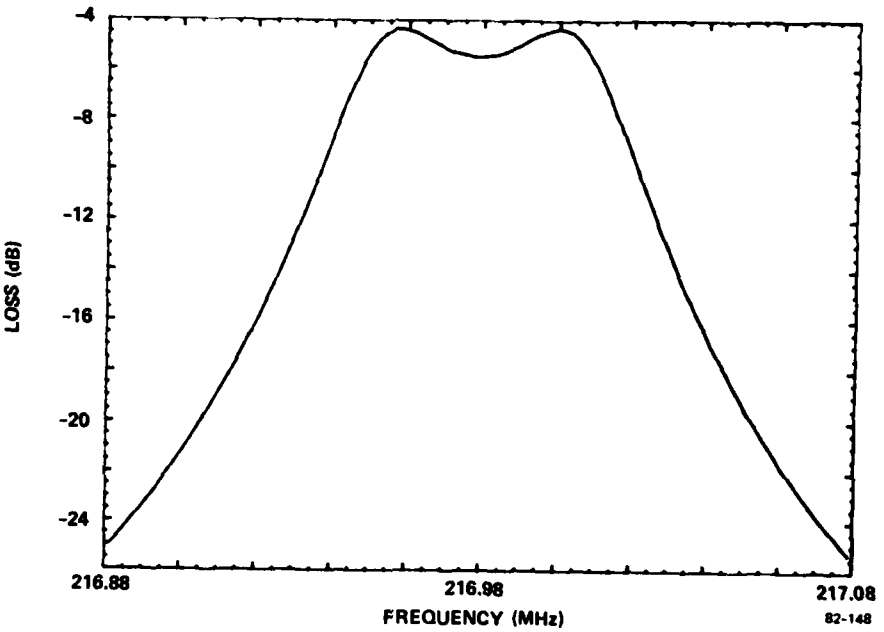

FIG. 20 Computed response of the acoustically-coupled cavities No. 1 and 2 (or 5 and 6) for D277, electrically unmatched into 50 Ω.

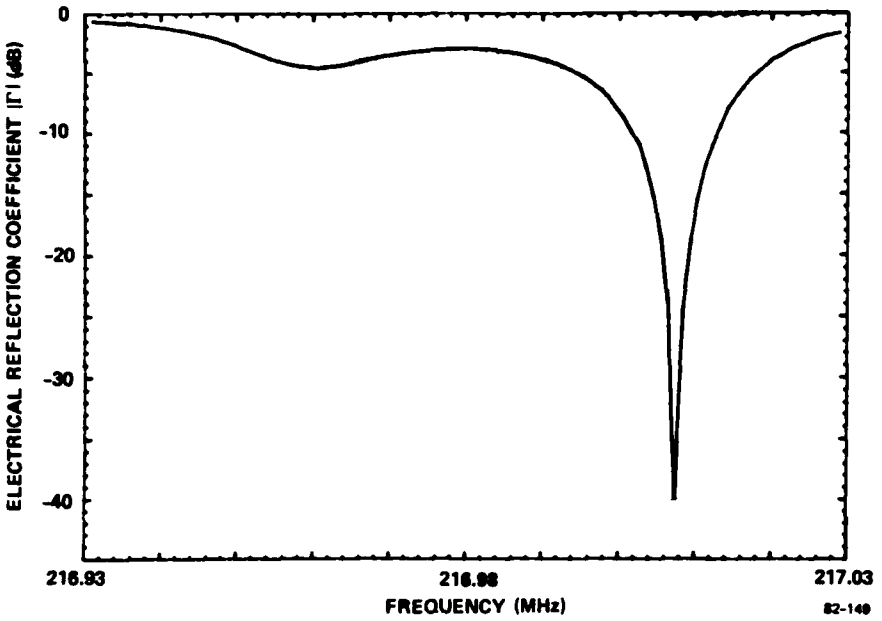

FIG. 21 Computed reflection coefficient magnitude, $|\Gamma|$, for cavity No. 1 of D277 (the input in the upper left of Fig. 2).

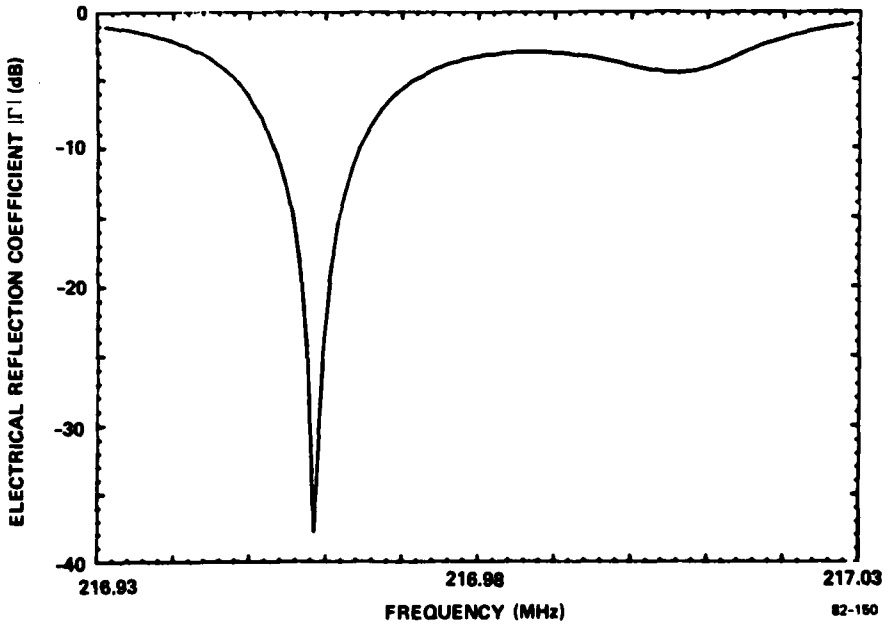

FIG. 22 Computed reflection coefficient magnitude, $|\Gamma|$, for cavity No. 2 of D277 with cavity No. 1 electrically unloaded.

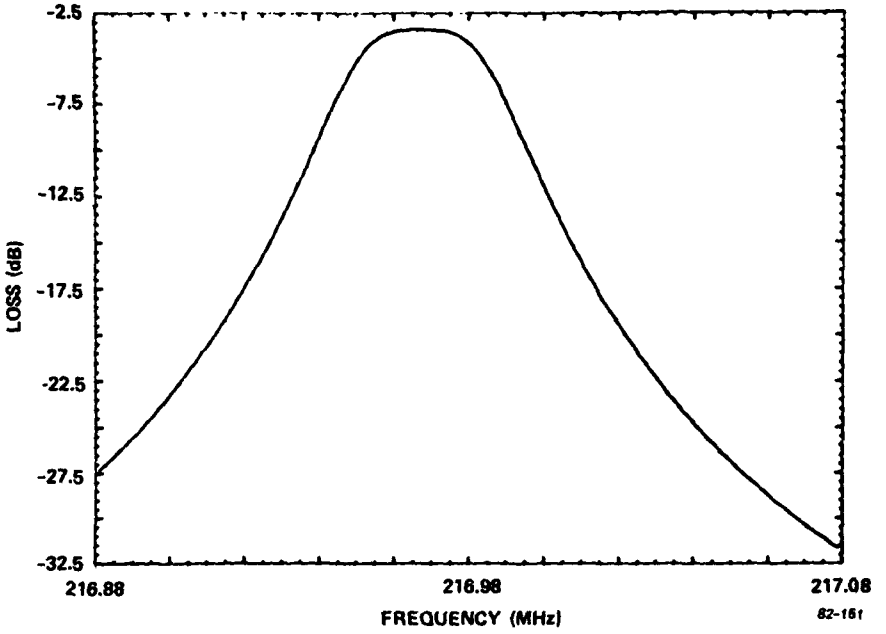

FIG. 23 Computed response of the acoustically-coupled cavity-pair (No. 3 and 4 of Fig. 2) for D277, electrically unloaded.

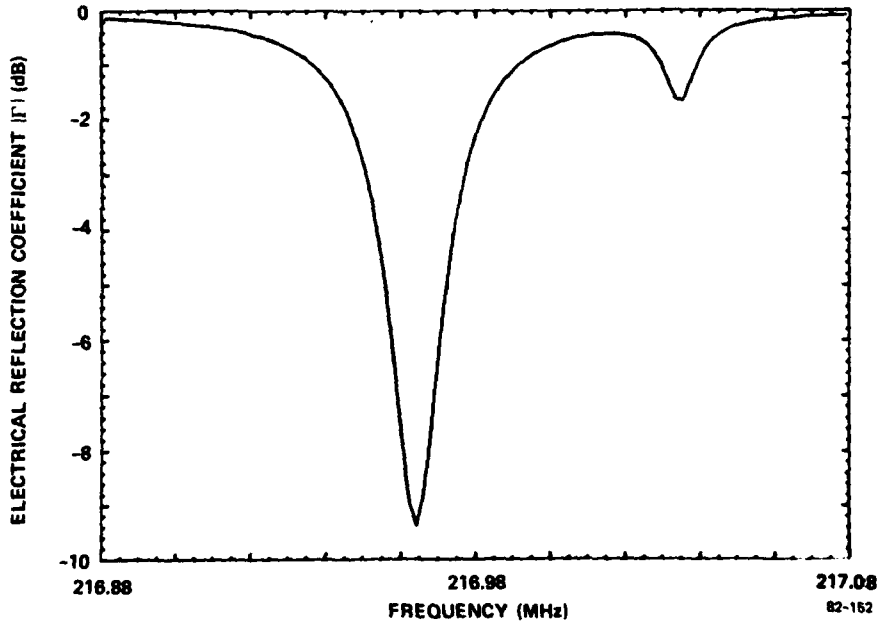

FIG. 24 Computed reflection coefficient magnitude, $|\Gamma|$, for D277 cavity No. 3 of Fig. 2 with cavity No. 4 electrically unloaded. Both cavities are at the same frequency.

This concludes our description of the synthesis and analysis procedures developed thus far in the program. In the following sections we detail the fabrication procedures and then present experimental results.

SECTION 3

DEVICE FABRICATION

We now describe the device fabrication process including substrate selection, design of the photomask, processing, trimming, and packaging. Only the essentials are covered here as many of the procedural details are lengthy and are already well known to persons skilled in the trade.

We have chosen to use two-inch diameter/.020" thick "ST" cut quartz discs as the substrate for each filter. Our goal is to fabricate all elements of the filter on a single substrate including resonators and capacitors. Any inductors necessary would have to be separate elements. The quartz discs were chosen for use because they are compatible with our mask aligner and we have more than adequate surface area for the complete device. Several suppliers have been used for this material and we have found that, first of all, discs of this size are very expensive (on the order of a hundred dollar each) if they do not include a "seed" crystal down the center, and secondly crystals with growth defects such as twinned zones and areas with high dislocation densities are sometimes received. Since we cannot fabricate a device on the seed because in general they will not function properly, we must know where the seed is and then make provision for placing the resonators elsewhere. This we accomplish by having the vendor outline the seed position on the unpolished side of the substrate. We then offset the filter sections on the mask so as to avoid the seed which is usually in the crystal center consisting of a long narrow strip parallel to the X axis. Frequently the seed edge is very pronounced and can be seen when properly held to the light. To further ensure that the quartz is adequate, we specify that all substrates are to be cut from the same stone, and we chemically etch one substrate from each lot in a solution of buffered hydrofluoric acid for a day or so. Imperfections in the crystal are clearly highlighted by this procedure. We had one lot of quartz of particularly poor quality and resonator sections, though not placed on the seed, were very often significantly different in frequency and Q value. In addition, thermal stresses, on

imperfect quartz, which occur during rapid (20°C)/Min) heat cycle would often cause a resonant section to shift upward in frequency by about 4 percent on this poor material. This indicated that twinning had occurred due to the propagation of dislocation from an already twinned zone. The crystals are also made with a flat about one inch long, which may be parallel or normal to the X-axis, to properly align the resonators with the X direction of propagation.

The photolithographic mask is produced by writing optical-pattern-generator flash instructions on a magnetic type an sending this tape to one of several mask houses. Since the resonators are fairly "regular", as are most surface wave devices, we have prepared computer subroutines which may be called to produce the flash instructions for a split-symmetric-transducer two-port device or a two-pole acoustically coupled pair. The subroutines are called with a relatively few number of arguments necessary to specify the structure. New mask designs are therefore implemented very quickly. In Fig. 25 we show a computer generated plot of a recent six-pole resonator design (D283). The circle (with two cords) is for alignment of the pattern on the disc, and the octagon surrounding the filter pattern is used to outline the saw cuts to be made when dicing the crystal. The octagon is sized as as to produce a crystal which fits properly in the header we have chosen. Further items of interest on the mask are the four interdigital capacitors, oriented horizontally to avoid an acoustic response at the resonance frequency, alpha-numerics to define cavities, etc., bonding pads, and a set of exposure blocks used in a second non-critical masking step during processing. For this relatively low frequency work in the VHF region we use iron oxide masks which are semitransparent. During processing we can see the substrate through the mask which facilitates alignment and allows us to ensure good mask-substrate contact. For higher frequency devices we must use low-reflectively chrome masks.

The device fabrication can be understood by reference to Fig. 26. We clean and bake the substrate, and coat the substrate with about 1 micron of AZ-1470 photoresist. As shown in Fig. 26 (a), the entire device pattern (transducers, reflectors, capacitors, bonding pads, etc.) is

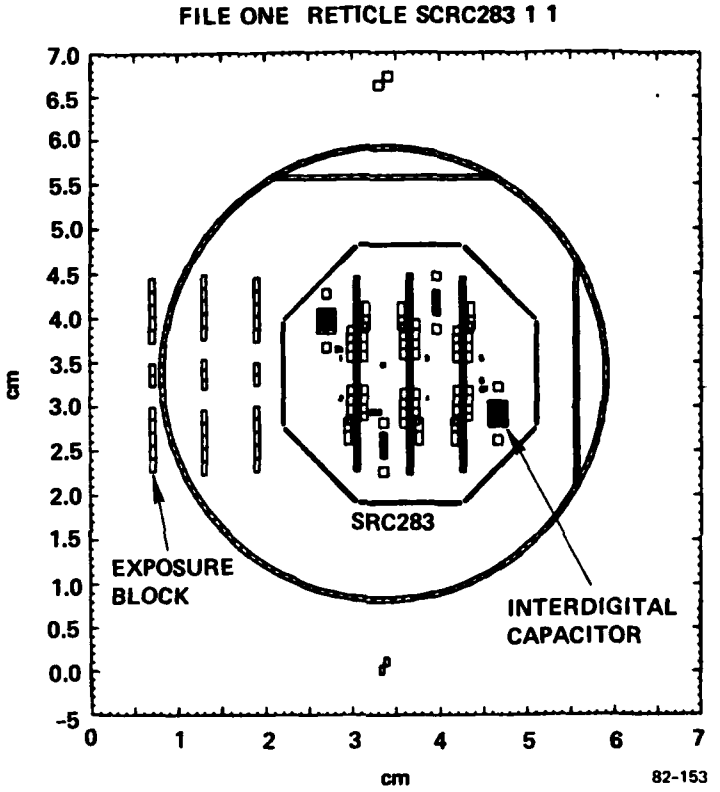

FIG. 25 Computer plot of a recent photo-mask for a six-pole resonator filter, design D283.

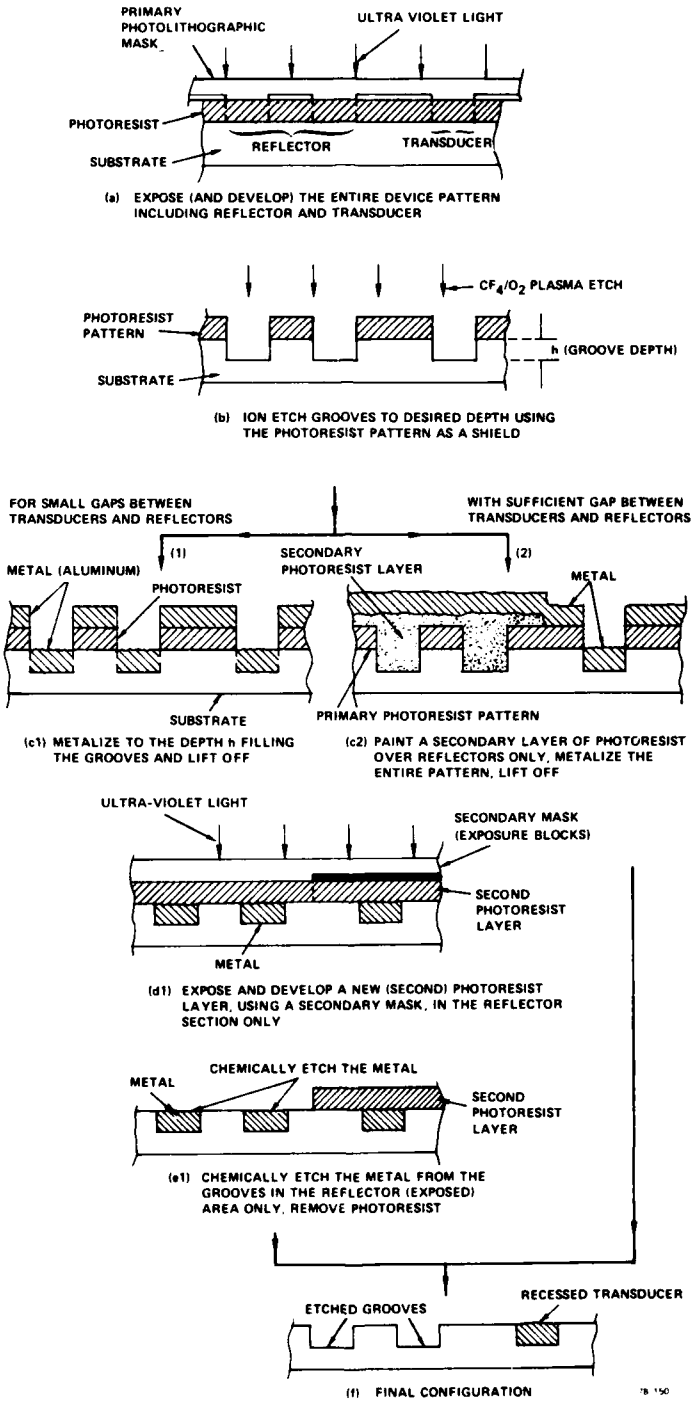

FIG. 26 Process steps required for fabrication of a recessed-transducer/ grooved-reflector resonator system.

exposed and the photoresist pattern is developed. The entire pattern is then reactively etched, at low power (~ .1 watt/cm^2) to prevent photoresist bake-on, in a RF sputtering station with a CF_4 (80 percent) plus O_2 (20 percent) plasma. This gas mixture is used because we obtain highly reproducible etch rates (± 3 percent) without stringent operating procedures. This is so because etching is produced primarily by a chemical reaction between the ions in the plasma and the quartz. For the D279 devices we etch to a depth of 2400 Å (.012 λ_o) and the D277 devices are etched to 1450 Å (.01 λ_o). After etching, the entire pattern is metalized with a bonding layer of chromium (100 Å) followed by aluminum (with about 3 percent copper to inhibit electro-acoustic migration of the electrode metal) thick enough to fill the grooves. This latter step is shown in Fig.2 6 (c_1). When enough space exists between the reflectors and transducers, we can follow step (c_2) and coat the reflectors with resist prior to metalizaton thus simplifying the procedure. However, for the devices in this program we kept the spaces small and therefore followed step (c_1) to improve our yield. Following metalization we then lift-off the unwanted metal, by immersing the substrate in acetone, yielding recessed transducers, and reflector grooves filled with metal (to be removed). After recoating the device with resist, we use the exposure blocks, seen on the mask of Fig. 25, to expose only the device reflectors and develop the resist away per Fig. 26 (d1). The metal in the reflectors may then be chemically etched away, using commercial aluminum and chrome etchants. For two-pole acoustically coupled cavities we only remove the aluminum. We leave the thin chrome layer at the base of the reflector grooves to act as a mask which allows us to selectively etch (in a CF_4 + O_2 plasma) the quartz (ridge tops) reducing the ridge height and the reflectivity of the structure. By this means, shown in Fig.2 7, we can increase the coupling between acoustically-coupled cavities after fabrication. Finally, we recoat the device with resist to protect the structures and dice the wafer to yield the octagonal substrate shown on the mask of Fig. 25.

The device is cleaned by removing the resist in acetone and by exposing the entire device to the CF_4/O_2 plasma in the RF sputtering station for about one minute. We have found this to be a very effective

cleaning procedure as evidenced by increased Q values following such exposure. The frequency of each resonator cavity is then found by using a set of microprobes. Each cavity remains isolated and no leads are bonded on until all cavities and reflectors are trimmed to specification. The resonant frequencies and two-pole pair responses are all measured, as discussed in Section 2, and recorded. The frequency of each cavity is then trimmed downward to the required value, and the reflector-coupling values adjusted as necessary.

To frequency trim each cavity, we selectively etch the quartz in a CF_4/O_2 plasma by RF sputtering. The change in device configuration is shown in Fig. 28. In this process the aluminum electrodes remain substantially unchanged (etch rate difference on the order of 10:1 are generally obtained) while the quartz is removed in a uniform manner. When performing this trim procedure, we shield all portions of the structure, using ungrounded metal masks, which we do not wish to expose to the plasma.

The etching process may be perfomed by RF sputtering or plasma-assisted etching, processes which are discussed Ref. 18, Sections II-1 and V-2, respectively. The gas mixture we use is CF_4 (80 percent) + O_2 (20 percent) by volume, though the percentage of O_2 is not critical, and our trimming is usually performed in an RF sputtering station with a backfill pressure of about 20μ (of Hg) at a power density in the range of 0.1 W/cm^2. We have successfully performed device trimming in a very simple barrel-type plasma reactor[19] though the trim rates are much lower than for RF sputtering. The etching of the quartz is performed by chemically reactive ions formed by disassociation of the CF_4. The function of the O_2 is to suppress fluorocarbon-polymer formation (which coats the device surface in the absence of O_2) and to enhance etching by the formation of an oxyfluoride (OF) species and by increasing the fluorine-carbon ratio. The frequency trim rate for a given device design is established empirically by subjecting a device to the etching process for a given length of time. We generally trim a device to frequency using an iterative procedure so as not to reduce the frequency below that which is desired. Also, the devices are designed and

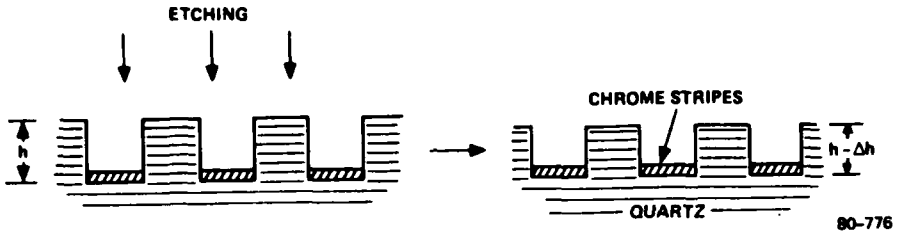

FIG. 27 Section view illustrating a technique for varying the coupling (by changing the groove depth) of grooved grating-couplers on quartz.

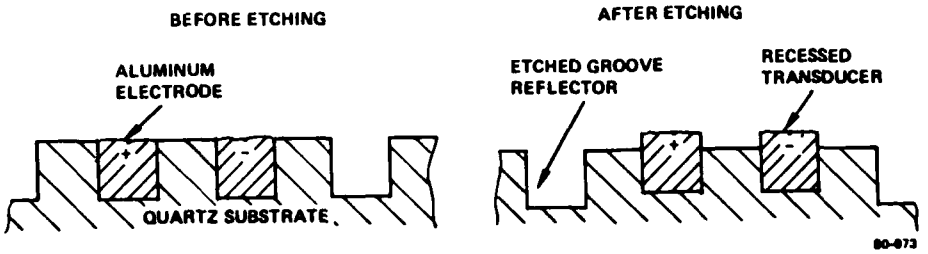

FIG. 28 Section view of the resonator configuration before and after selectively etching the quartz substrate in a tetrafluormethane (CF_4)-plus-oxygen plasma.

fabricated to have an initial frequency higher than the final frequency desired. The maximum trimming range for resonators being made is approximately 500 parts-per-million. This range is adequate to compensate for the maximum device-to-device frequency variations of several hundred ppm we experience for our devices. Our photomask designs and fabrication procedures allow consistent attainment of an initial device frequency close enough to the desired frequency such that this trimming procedure may be successfully applied. We can trim our cavity resonance frequencies to an accuracy of 5 ppm which calculations show is acceptable for the filters under consideration here. The dominant effect of increasing the transducer step height for resonators is to increase the surface-wave reflectivity of the electrodes. A downward shift in the cavity resonance frequency occurs due to the stronger interaction between the waves reflected from the transducers and those reflected by the reflectors as the transducer reflectivity is increased. There is also a downward shift of the surface wave velocity under the transducer, however, calculations show that this has a minor effect on resonator cavity frequencies. This trimming process is discussed in more detail in Ref. 10. For the devices in this program, we have found the trim rates to be in the range of 0.2 kHz/sec of etch which is slow enough to allow for very good control.

In trimming the reflector to adjust inter-cavity coupling we initially etched only the coupling reflector and shielded the outer reflectors (which also had the chrome removed). We found, however, that the rejection of these two-pole structures degraded significantly. By modeling the devices on the computer we were able to duplicate the experimental results and by calculation we found that etching all three reflectors eliminated this degradation. What happens when only the center reflector is etched is that the symmetry of the each cavity is broken in large measure due to the change in the phase, ϕ, of the reflection coefficient for the center reflector. For long transducers we rely on a symmetric system to suppress the M±1 (where M is the mode number for the resonance) longitudinal modes, and these modes increase in level degrading the rejection when the symmetry is destroyed. Thus we leave the chrome in all three reflectors and etch all three together, while shielding the transducers, as needed to attain the necessary coupling.

After the device has been fabricated and all cavities and reflectors trimmed to specification, the leads (one mil aluminum wire) are bonded to connect all structures as desired. Ideally we would connect the coupling and matching capacitors per Figs. 1 and 2 and place a small THINCO[20] inductor (using an epoxy adhesive) on the substrate as well. If any adjustments were still required one could laser trim the capacitors (we would generally make the capacitors somewhat larger than per design) to yield the desired response. The filter would then be monolithic except for the inductors. In practice we could not carry this plan out, however. First of all we had no laser-trimmer convenient for our purposes, but more importantly we did not know our design parameters accurately enough (particularly k^2 and parasitic capacitance) to predict what was required. Thus, we were forced to experiment with different values of coupling and matching components to see which produced the desired response. Also to add flexibility, we placed the input/output matching L and C's on a circuit board external to the package and experimented with inductors in place of the coupling capacitors. We also split two devices into three separate sections, mounted them in separate headers, and placed the headers in circuit boards which allowed adjustment of the coupling components. We note here that once a device is fabricated with matching/coupling components on the substrate and leads bonded on, it is almost impossible to make a change without degrading the performance of the device. This is so because bonding leads often becomes impossible, and working with adhesive or silver paint (for lead bonding) inevitably contaminates these very sensitive devices irreversibly. For each device response to be discussed in the experimental section we shall indicate how the device was configured.

The completed substrates were then bonded to the heavy lead-pins of the Type D[21] (1.3" diameter) header shown in Fig. 29 using a gold filled epoxy[22]. The aluminum leads were then epoxied to the appropriate header pins, and a lid was cold-welded to the header in a high vacuum ($\sim 10^{-7}$ torr). The first serious problem we ran into in this procedure was that the substrates were subjected to varying levels of stress due to the fact of being rigidly bonded to a header with the lid sealed on.

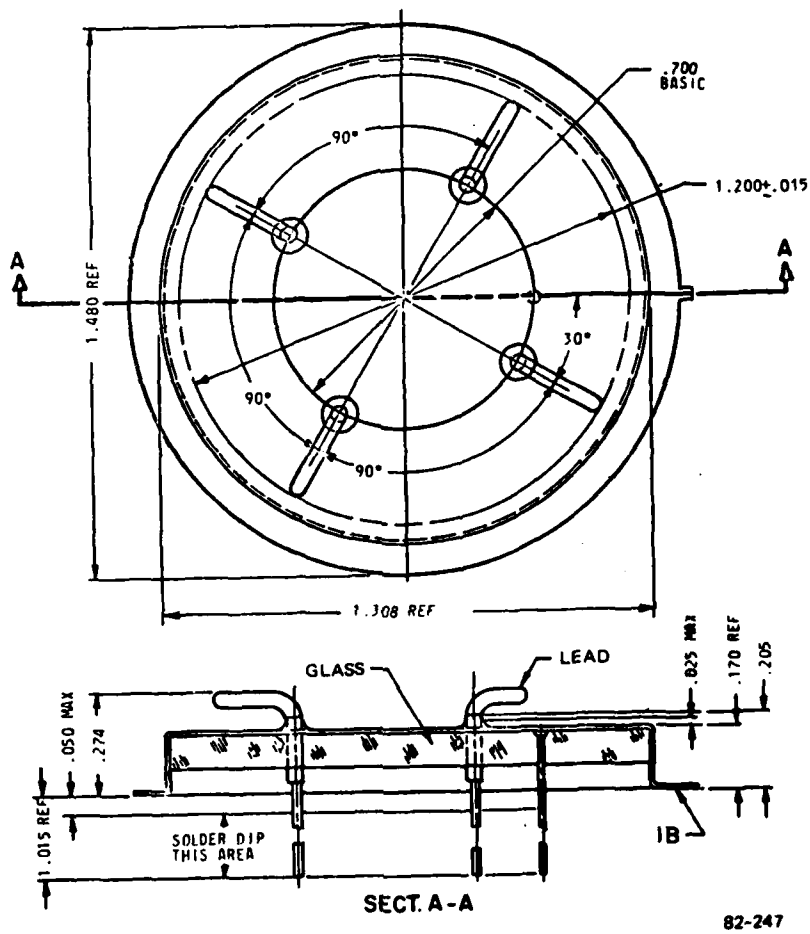

FIG. 29 Diagram of the cold-weld-sealable Type D leader.

These stresses manifested themselves as a degredation, or complete disappearance, of the filter response. We found that the filter response could be made to vary by thermal changes or by mechanically stressing the sealed header. The only cure we had for this was to "nibble"[23] the lip of the header off thereby removing the lid and relieving the stresses. It turns out that the header and the lid may not both be perfectly planar where they join. The lid, being more rigid due to its structure, forces the header to conform to he shape of the lid lip when the seal is made in the press. On some devices the resulting header distortion so stressed the substrate that the device failed to work. We did not find these things out until we were sealing our devices for delivery at the end of phase I since we were just able to bring everything together (cold-weld-sealing, device fabrication, etc.) in the final month. We lost several devices right at the end due to irreversible damage before we discovered the nature of the problem. In addition, several of the devices delivered had their lids removed to relieve the stresses, and then the lids were replaced by soldering in several spots to act as a dust cover. To summarize this, we shall in all future devices mount the substrate on three flexible mounting structures which are to be bonded to the header. The height of the mounts will be such as to place the substrate to just above the header pins (Fig. 29) but the mounts will prevent header stresses from being transmitted to the substrate.

The second problem we found in cold-weld sealing the packages was that they had vacuum leaks where the leads penetrated the glass seal. We recognized this problem late, also, so the only thing we could do was to place epoxy around the lead at the glass interface on the outside where the lead exits the header. With this fix we were able to ship one device with a tight vacuum seal, the remaining devices are all operating in air. We believe that the leaks resulted from the same stresses which caused the filter responses to degrade, namely, the header distortion when sealed. With the substrate mounted to the pins, the header stresses are transmitted to the substrate via the glass seals. This problem will be investigated thoroughly in the next phase. Vacuum sealing is important in order to maintain device integrity by keeping out moisture, reducing aging by keeping out contaminants, and to reduce the insertion loss. Experimentally we find that the filter loss increases by 1.5 to 2 dB, for D277 or D279, when the vacuum seal is broken.

SECTION 4

EXPERIMENTAL RESULTS

We now present the filter response characteristics for the ten devices delivered (five D279's and five D277's), the responses of a "sectioned" filter, and a discussion of each device. Device response curves were sent to NRL as well as two matched circuit boards (one for each of the two designs) and photographs of several devices. Here we shall include a photograph of several devices plus a description of the circuit board and additional response curves where these are useful.

Type II - D279 Filters

All five of the D279 filters delivered worked reasonably well except for the general lack of good out-of-band rejection. Only one of the filters, D279-8, is vacuum sealed, all others either have leaks at the pins or have had the lids removed and soldered back on. The filter response curves were taken with an unmatched test board, that is with $L_I = L_O = 0$, $C_I = C_O = 0$ (referring to Figs. 1 and 2), and in a matched test board $L_I = L_O \sim 100$ nh (11 turnes of No. 24 wire .080" inside diameter) and $C_I = C_O$ are variable 0.8 to 8 pF[24] capacitors. The test boards have five receivers to mate with the five pins on the header, and OSM type connectors for the input and output ports. The capacitors are screwdriver adjustable with increasing capacitance obtained as the slug is turned inwards. All the devices match with only a small amount of capacitance (slugs turned most of the way out) and the boards for D279 and D277 are the same.

The response of D279-8 is shown unmatched in Fig. 30 and matched in Fig. 31, with the device photograph in Fig. 32, and the response of the unconnected filter sections in Fig. 33. This device had no capacitors connected between sections ($C_{12} = C_{34} = 0$ in Fig. 1), nor were the end capacitors on the substrate connected in. In Fig. 32 we see the method of mounting, and a leakage-suppression septum extending between the upper-right and lower-left (both grounded) electrodes. The input terminal is on the upper-left and the output on the lower-right. The unmatched

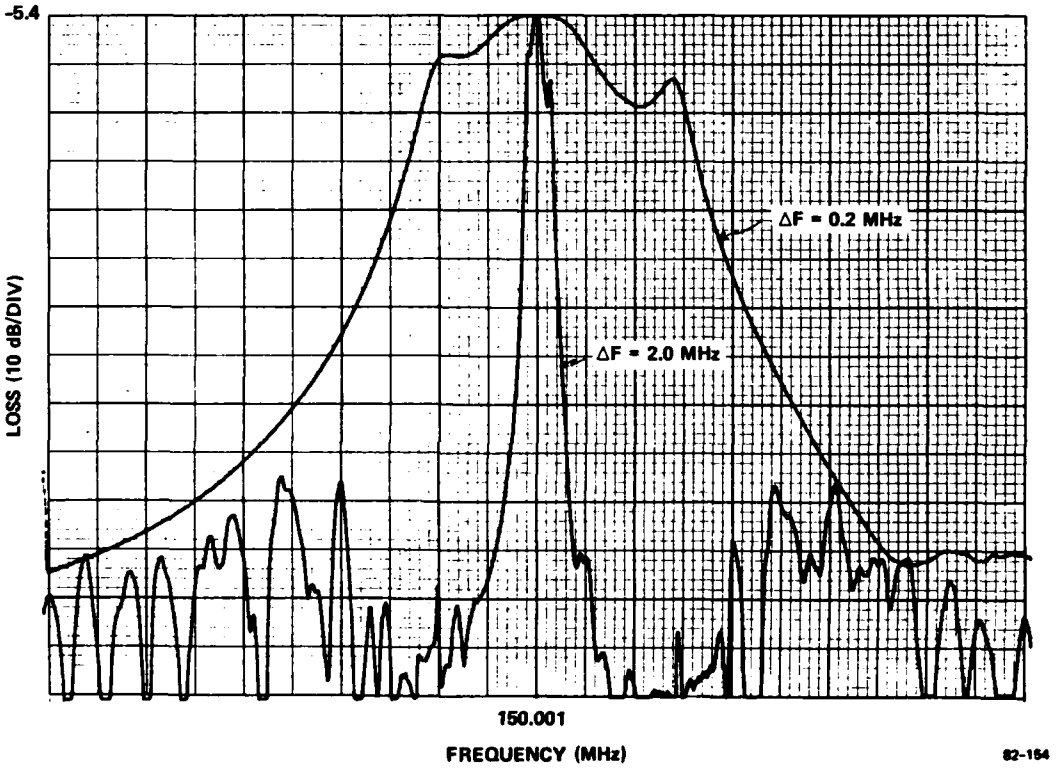

FIG. 30 D279-8 unmatched frequency response in vacuum.

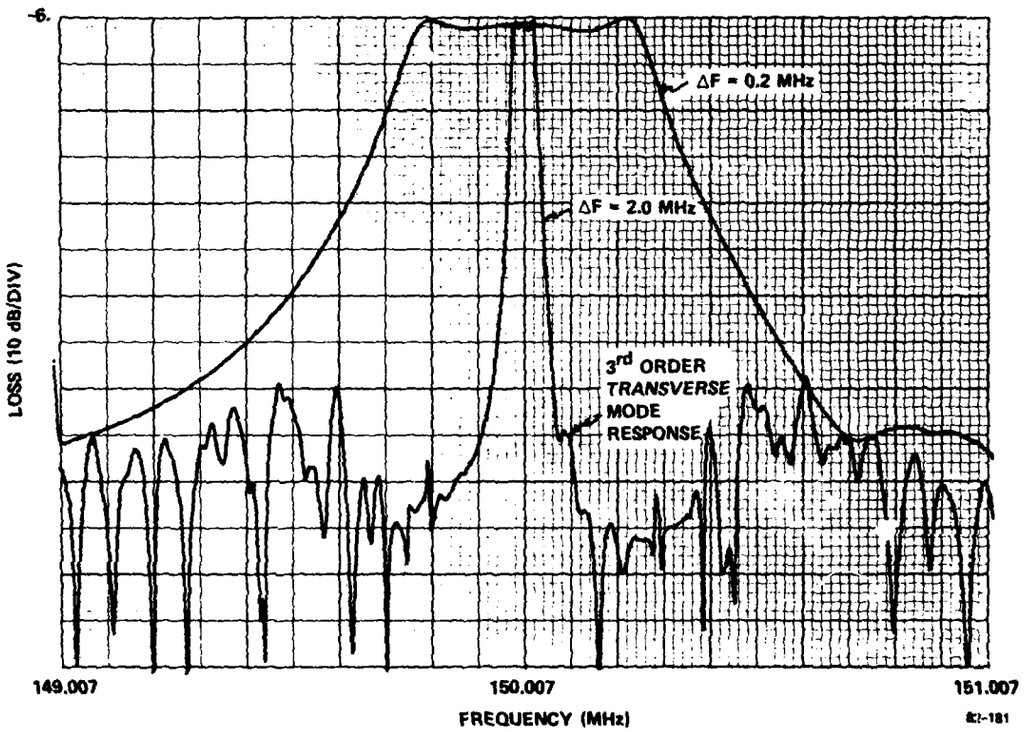

FIG. 31 D279-8 matched frequency response in vacuum.

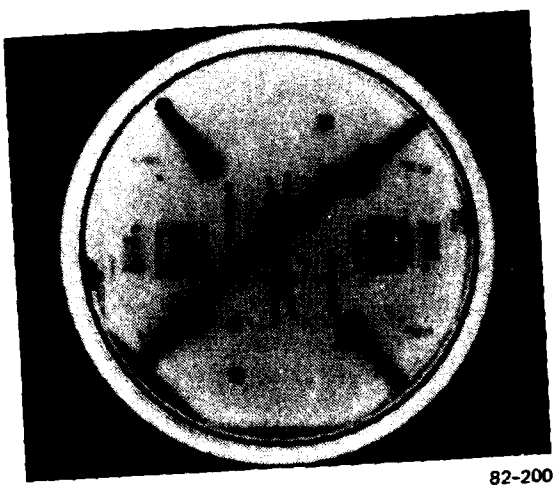

FIG. 32 Photograph of D279-8 prior to sealing.

response is notable for its coarse bandpass and for the rejection level of about 48 dB. The matched response (Fig. 31) has a 3 dB bandwidth of 50 kHz, a two dip bandpass (~ 1.0 dB), and 6.0 dB loss. In comparison with theory (Fig. 7) this response is 4 dB higher in loss and has one more dip than predicted. The bandwidth is relatively close, however. The matched rejection level is only 40 dB, much poorer than the 60 dB predicted. Extrapolating the response on Fig. 31 to the 60 dB level the bandwidth there would be about 250 kHz yielding a shape factor of about 5, close to the predicted value of 5.2. The curves of Fig. 33 show the response, before connecting together, of the two single-pole sections, cavities 1 and 4, which show about 20 dB rejection, 2 dB loss and a small third order transverse mode response about 100 kHz above the main resonance. The two-pole section, cavities 2-3, again shows about 20 dB rejection, a third order transverse mode response, and a dip of 1.5 dB versus the required response of Fig. 12. This overcoupling more than likely has caused the extra dip in the response of Fig. 31. Prior to another iteration of the four pole filter we must analyze the scheme of Fig. 1 to see whether or not we can improve the rejection level. The direct-electromagnetic-feedthrough (leakage) level is also rather high at about -70 dB from the passband level. This high level is due to the packaging, mounting in the circuit board, and the configuration of the board and the external matching circuitry. We are engaged in an ongoing effort to reduce the leakage and thereby improve the ultimate rejection-level of the response. We could also try improve the rejection close in by weighting all the reflectors to reduce the reflector sidelobe levels, however, they may not be possible for these 150 MHz filters because we barely have enough space in the package now and weighted reflectors would have to be somewhat longer requiring more space. We note finally that the third order transverse mode response in Fig. 31 is not very strong and could easily be tolerated, however, we shall reduce the aperture from 48 to 40 λ_0 on future designs in order to suppress this effect more completely.

In Fig. 34 we show the response of D279-7 which has a skewed passband, about 37 dB rejection and a 3rd order mode at -42 dB. This response is inferior to that of Fig. 31, and we again note the poor rejection.

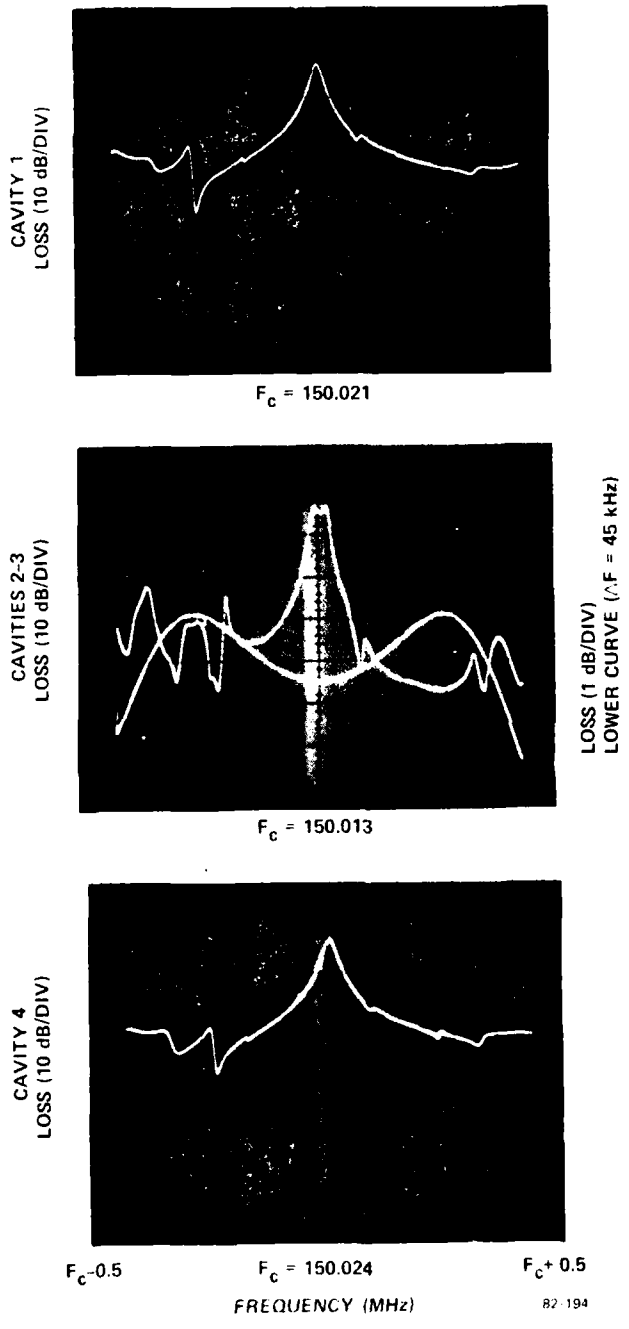

FIG. 33 Response of each filter section for D279-8 before interconnection.

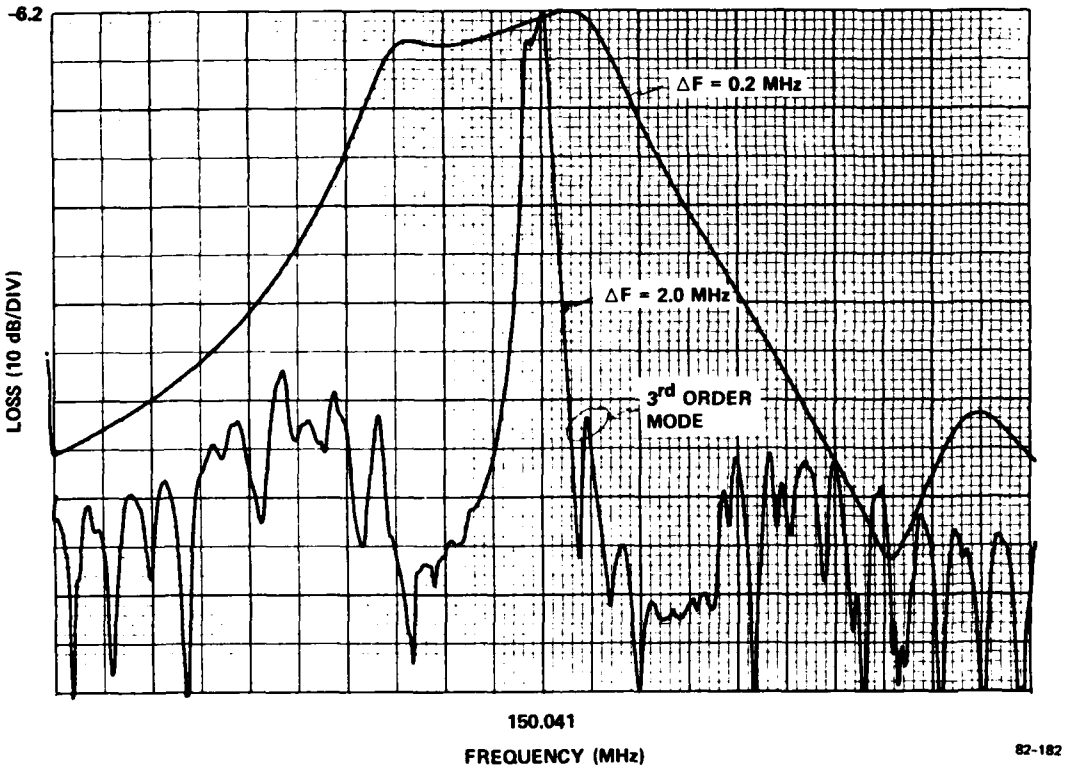

FIG. 34 D279-7 frequency response, matched, in vacuum.

Inspection of Fig. 35, where we see the response of each filter section, shows high quality resonances for cavities 1 and 4, but a strong (M-1) longitudinal mode for cavities 2-3 as well as a highly overcoupled (2.5 dB dip) response. In Fig. 36 we show the reflection coefficients measured for cavities 2 and 3, which we see are similar to that required theoretrically in Fig. 13, and note that the frequencies of the lower resonances are within 3 kHz of one another at about 149.982 and 149.985 MHz. The frequencies of cavities 1 and 4 were to be 2 kHz higher than those of Fig. 6 and they are actually about 6 kHz higher. We cannot attribute the poor passband response of Fig. 34 to this relatively small frequency difference. The case for this device leaks air around the pins so a measured response will be about 1.5 dB higher than the 6.2 dB shown on Fig. 34.

The response for D279-9 is given in Fig. 37 where we see a somewhat skewed passband, though not as bad as Fig. 34, a 6.6 dB loss, and a 43 dB rejection level. This level somewhat better than earlier devices but still not a real improvement. The responses of each filter segment are similar to those of Fig. 33. The isolated resonance frequency of cavities 2 and 3 are, however, about 10 kHz lower than desired. The case for this device leaks around the pins so a measured response in air would yield about 8 dB loss.

The response of D279-11 is shown in Fig. 38 where we note a vacuum loss of only 4.9 dB. This is one of the devices for which we had to remove the lid to relieve the sealing stresses discussed earlier, and the device is now not under vacuum but has the lid soldered on at several points. Measured loss under present conditions is about 6.5 dB. The 3 dB bandwidth is only 29 kHz compared to the 37 kHz desired and the rejection level is a poor 34 dB. Inspection of the sectioned response (not given here) shows rather high sidelobes (at -12 dB from the passband) of the transmission response for cavities 2-3, and we may attribute the high sidelobe of Fig. 38 to this cause.

The response for the final Type II device delivered, D279-10, is given in Fig. 39. We note the high loss of 14.6 dB (this device had its lid

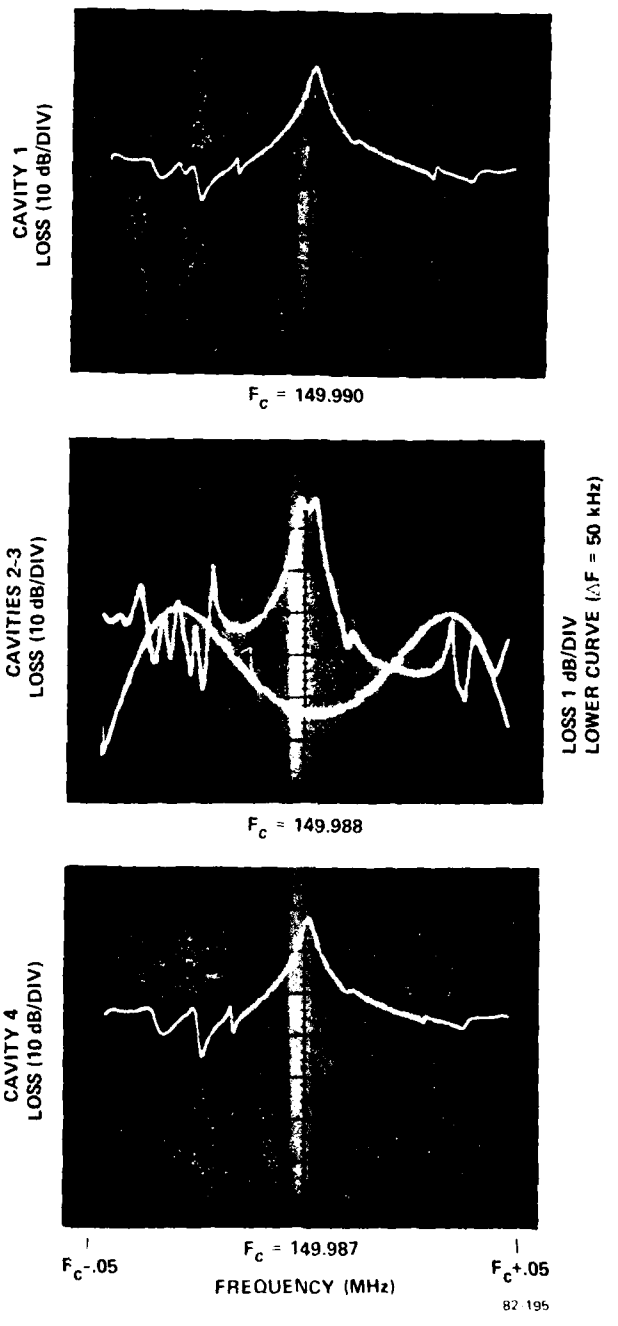

FIG. 35 Response of each filter section for D279-7 before interconnection.

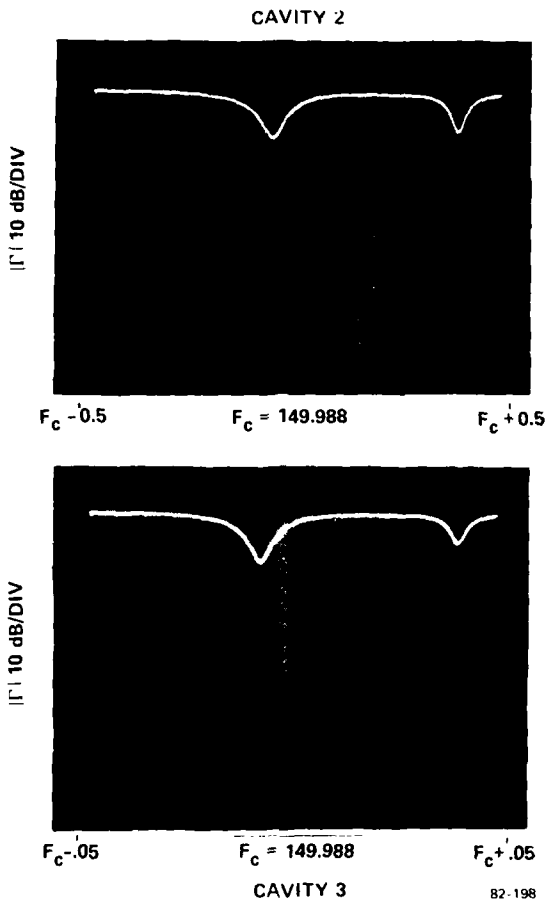

FIG. 36 Electrical reflection coefficients, $|\Gamma|$, for cavities 2 and 3 of D279-7.

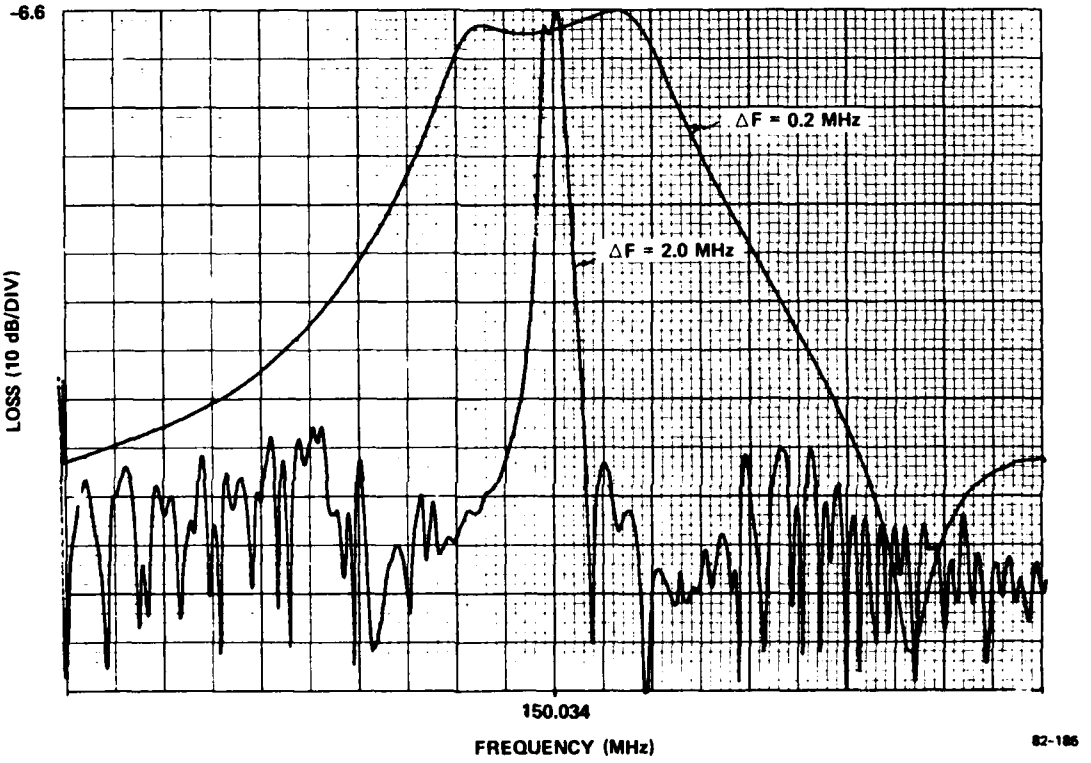

FIG. 37 D279-9 frequency response, matched, in vacuum.

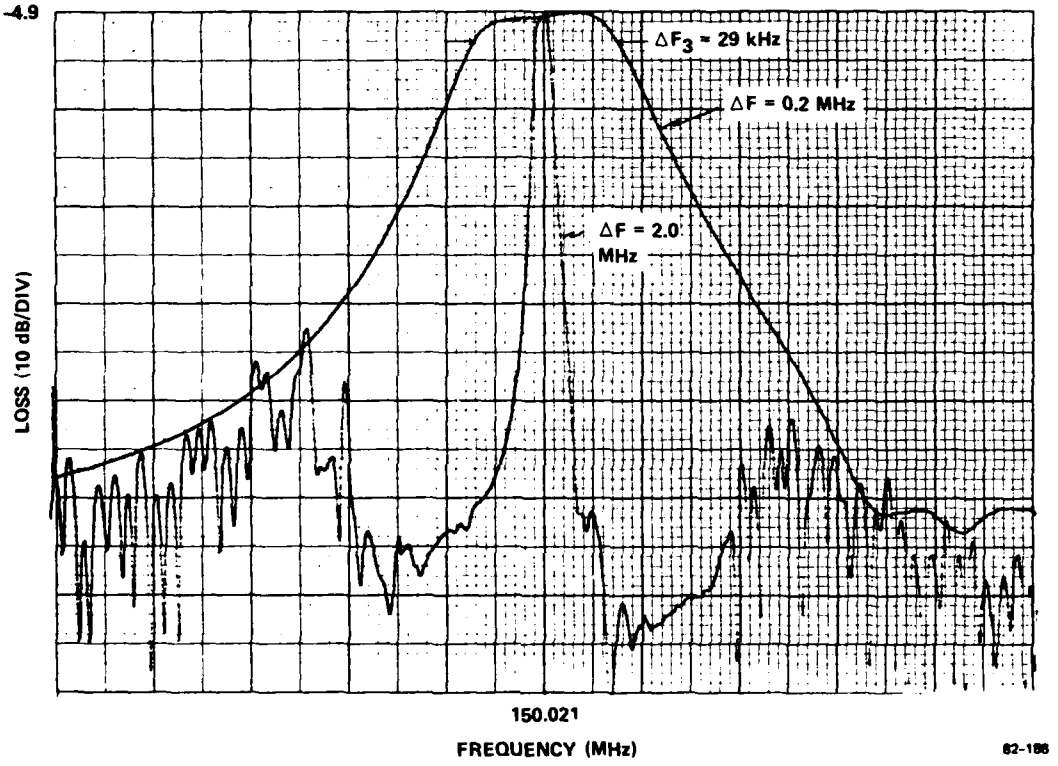

FIG. 38 D279-11 frequency response, matched, in vacuum.

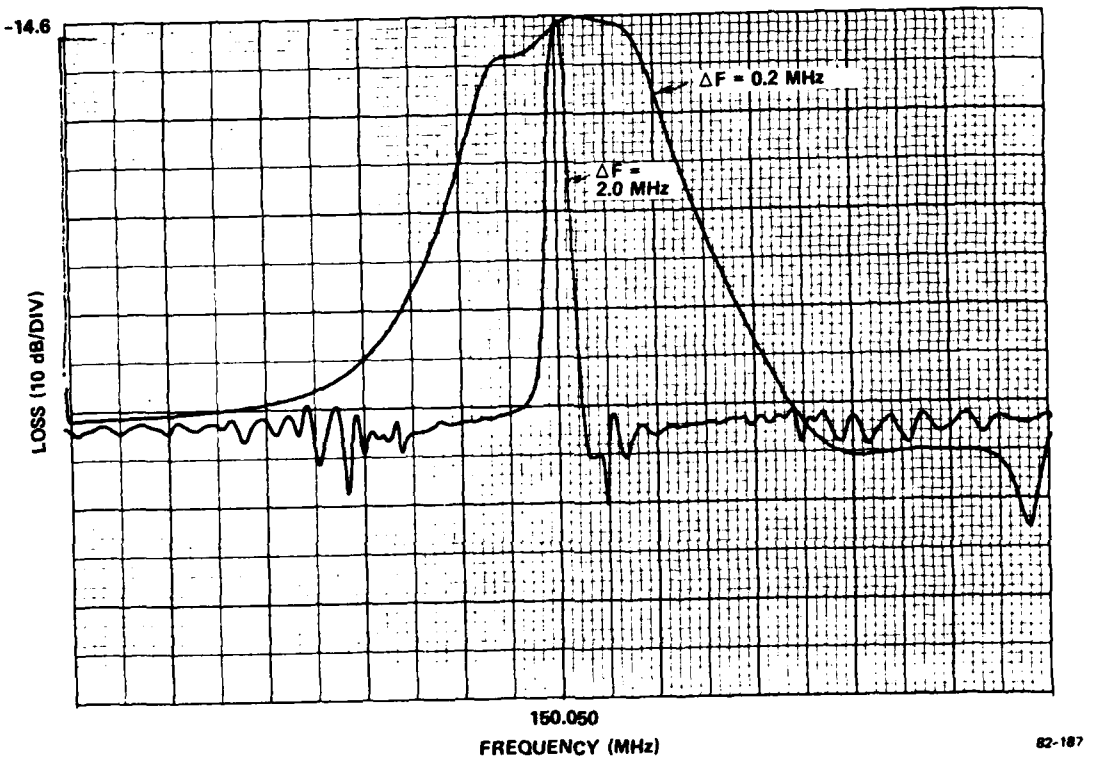

FIG. 39 D279-10 frequency response, matched, in air.

removed due to stress problems and the lid was soldered back on) and poor passband response. Inspection of the section responses (not given here) show that they were almost exactly as required, so we attribute the poor response to damage suffered in subsequent fabrication.

To summarize the results for the D279 (Type II) devices, we have found that the actual loss is 3 to 4 dB higher than theoretical but still close to the desired maximum of 6 dB. This additional loss can result from contamination during assembly (after trimming), unaccounted for parasitics, imprecise matching/coupling, an inaccurate model, device frequency inaccuracies, and inherent cavity Q variations. Our best guess at this time is that the parasitics, matching/coupling, and model errors are dominant causes of this loss discrepancy. The rejection levels were disappointingly poor being on the average only 40 dB close in and about 70 dB further out, due to leakage. The 40 dB rejection is 20 dB poorer than predicted and part of this discrepancy is probably due to the use of weighted transducer versus unweighted structures in the model. Since we desire 60 dB rejection, and experimentally we almost never meet theoretical prediction, we must conclude that the design D279 is inherently deficient and we must seek modifications to improve the theoretical rejection level. We believe we understand the problems encountered in fabrication and packaging with regard to stresses, but we must work to find the source of the leakage and work to reduce it. We shall try better case grounding, isolation of the matching components, and separating the sections into separate packages to gain knowledge of this deleterious effect. Finally, the passband responses differ significantly from the theortecial curves and we believe this is due largely to improper matching/coupling components.

Type I - D277 Filters

The first of the Type I, six-pole, filters we shall discuss is D277-13 the response for which is given in Fig. 40. The passband is rather coarse and does not meet the Butterworth response specified, but the minimum loss, in vacuum, is only 5.7 dB. This loss is only 1.4 dB greater than theoretical (see Fig. 15) and is considerably less than the 10 dB specified. The rejection is about 50 dB matched (about 60 dB unmatched) which is 25 dB less that predicted in Fig. 16. This rejection discrepancy

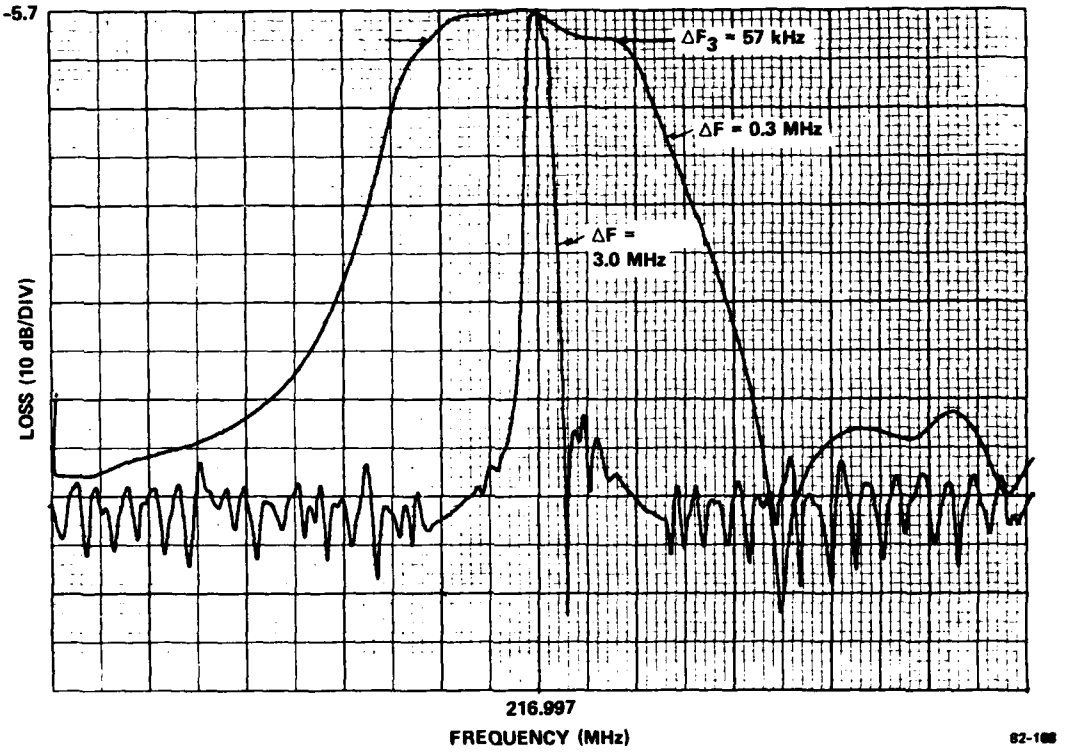

FIG. 40 D277-13 frequency response, matched, in vacuum.

is approximately the same as for the D279 filters. The leakage level is about -60 dB and probably for the same reasons as with the D279 filters. A significant third order transverse mode, at -42 dB, response occurs at 140 kHz above the resonance frequency. This device had 1 microhenry inductors coupling cavities 2-3 and 4-5 and these are clearly seen in Fig. 41 which is a photograph of this device. We also had stress related problems with this device and had to remove the lid and solder it back on to regain the response. The loss is in air and is about 7.5 dB. The response of each isolated section is shown in Fig. 42 and these may be compared with Fig. 20 (for cavities 1-2 and 5-6) or with Fig. 23 for cavities 3-4. The deviations from the ideal are not too large, but the resonance frequency of cavities 3-4 is about 10 kHz above that required for an optimum response. The reflection coefficent data for each cavity is given in Fig. 43 and may be compared with Fig. 21 (cavities 1 and 6) Fig. 22 (cavities 2 and 5) and Fig. 24 for cavities 3 or 4. The agreement in form is reasonably good but the magnitudes are very sensitive to losses and agreement on this point is more difficult to achieve.

The response of D277-8 is shown in Fig. 44 where we see that the loss of 10 dB just meets specification and the bandwidth of 65 kHz exceeds the required value. The passband is not a smooth Butterworth, however, and the irregular shape will yield an irregular shape phase response. The filter-to-filter phase response is to be within 10° for these Type I devices and as we see thus far the irregular passbands indicate that this phase requirement is going to be difficult to meet. Unfortunately we did not record the phase responses prior to shipment. This response was recorded with the device in vacuum but the case leaks around the pins and the loss measured now will be about 11.5 dB. The rejection level is about 45 dB, somewhat poorer than D277-13 but still better than any of the D279 series filters.

The response of D277-10 in Fig. 45 shows a loss of 12 dB (13.5 in air) and a rejection of about 45 dB. The leakage level is higher on this device than on D277-8 or D277-13 for reasons which are not understood. We encountered stress related difficulties with this device and so were forced to remove the lid and replace it by soldering. The relatively high

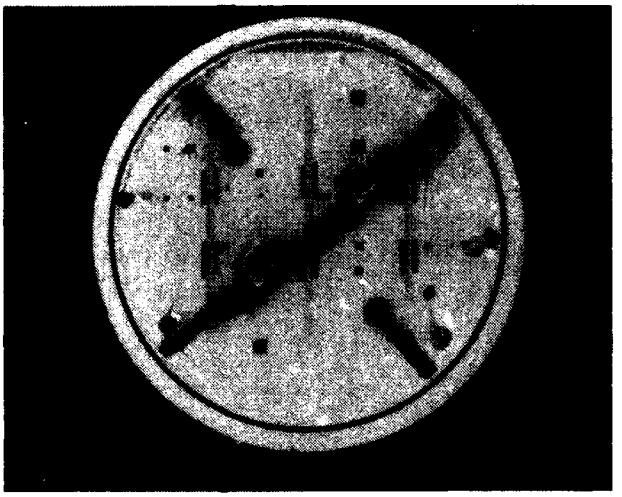

82-248

FIG. 41 Photograph of D277-13 prior to sealing.

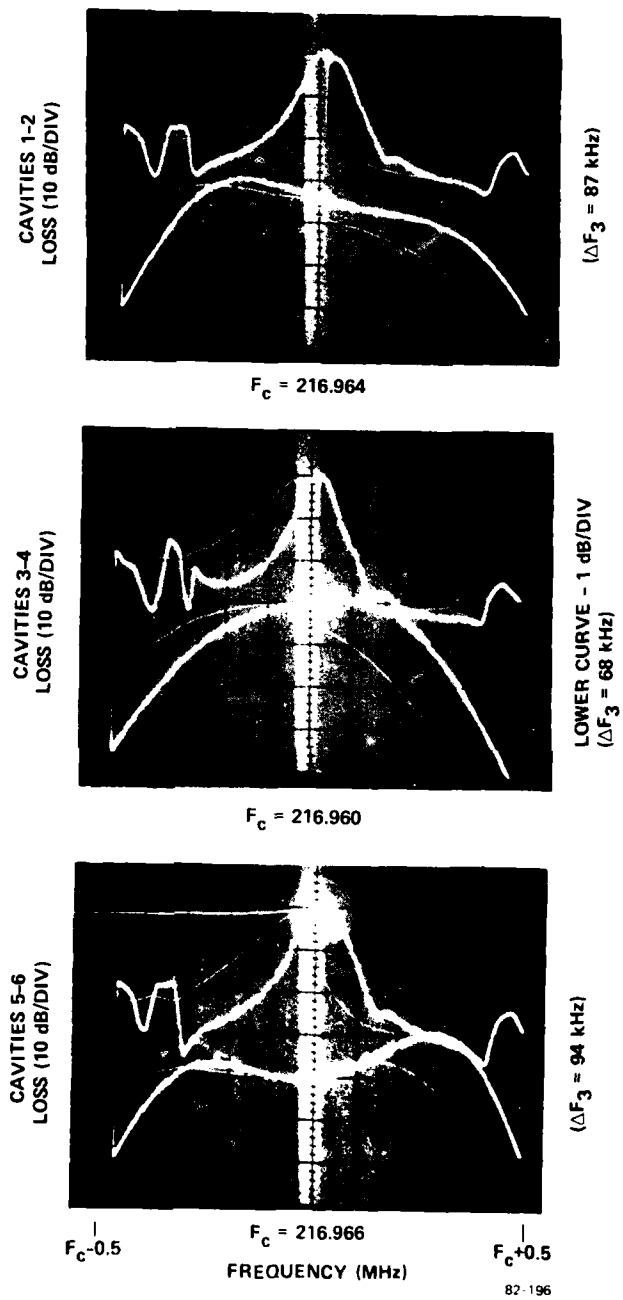

FIG. 42 Responses of each section of D277-13 taken in isolation.

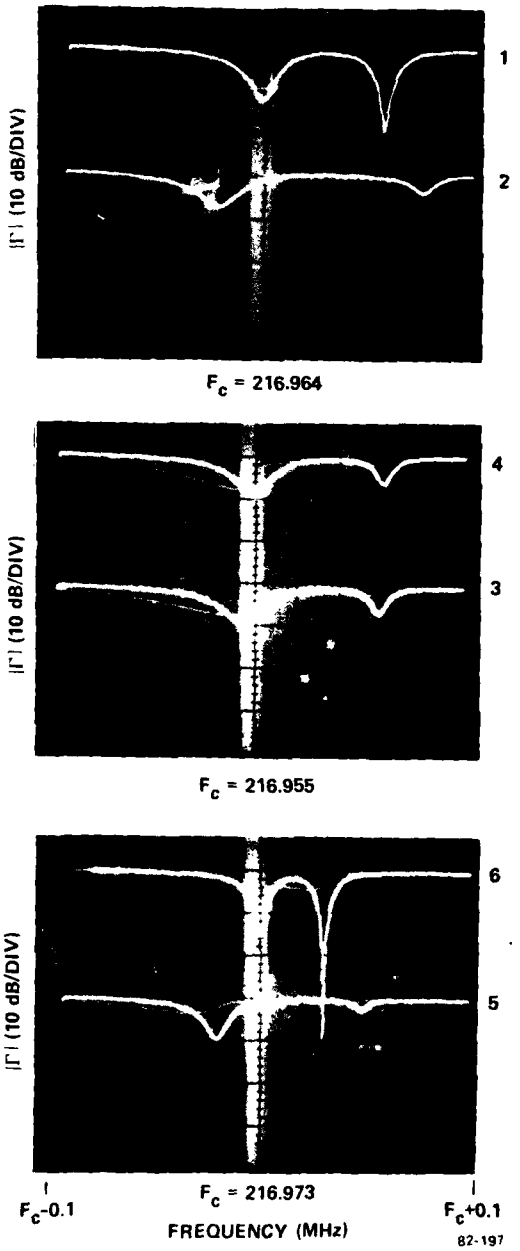

FIG. 43 Electrical reflection coefficients, $|\Gamma|$, for each cavity in D277-13. Cavity numbers are on the right margin, and the levels are offset for presentation.

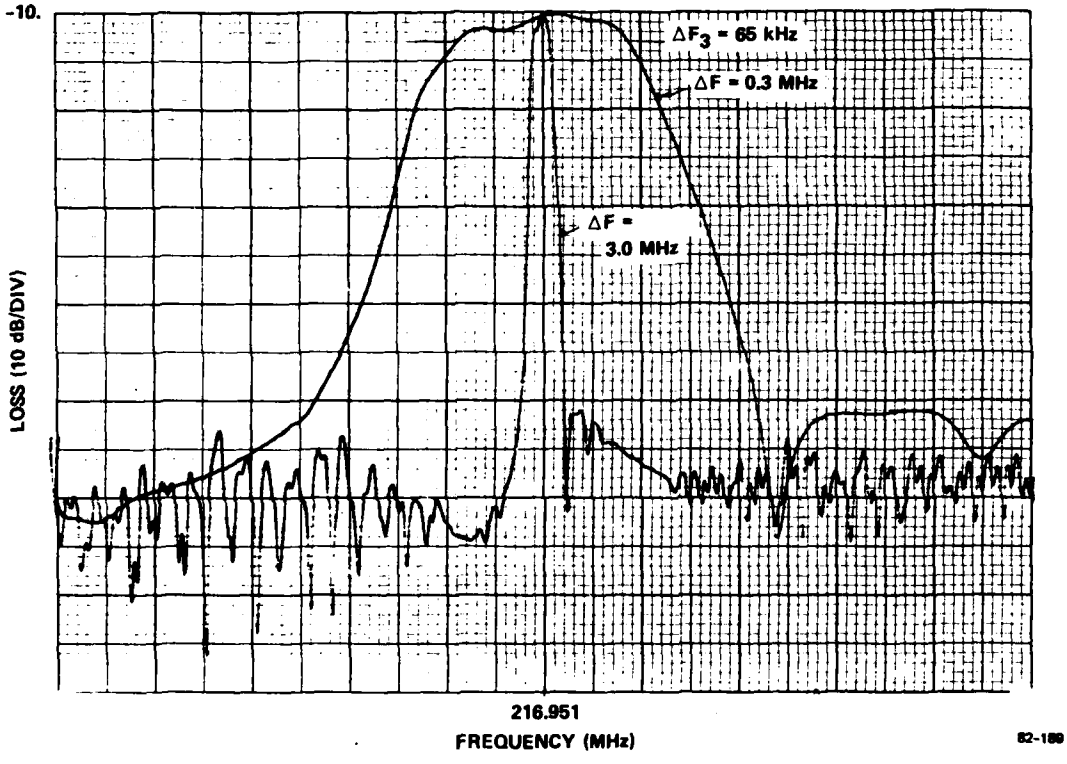

FIG. 44 D277-8 frequency response, matched, in vacuum.

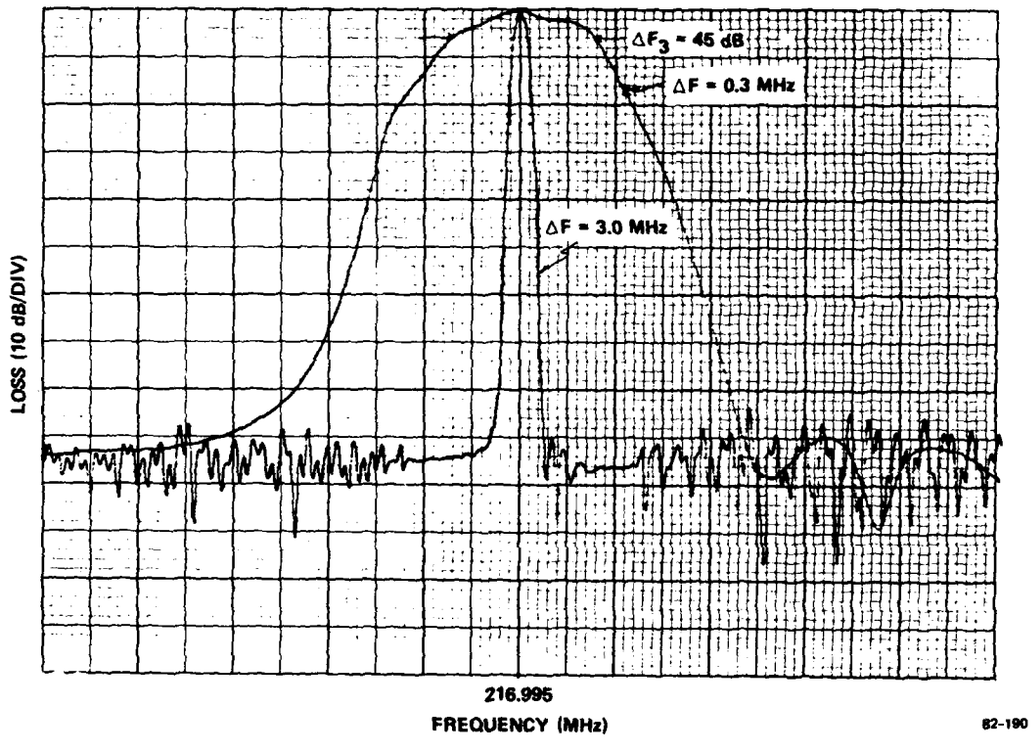

FIG. 45 D277-10 filter response, matched, in vacuum.

loss cannot be explained for certain because, in isolation, each section was trimmed properly and had low loss.

Devices D277-9 and D277-11, the responses for which are given in Figs. 46 and 47 respectively, are basically non-functional devices and were shipped to NRL only because we had a low device yield and we ran out of time to deliver. In both devices the cases leak around the pins and so they are not vacuum sealed. Also, the reason the responses are so poor is that we had much difficulty in bonding the leads and were forced to use silver paint or conductive epoxy just to make the devices work. These bonding agents frequently cause difficulty with contamination. As can be seen from the device numbers, we actually made 12 or 13 of each type (277 and 279) to get the five needed for delivery. In future work we believe that we can improve the yield substantially, however, as a result of the lessons learned.

Another device D277-6 was diced so that each section (cavity-pair) could be encased alone, and then the three cases placed in a matched circuit board with facility for easy replacement of coupling components. The response obtained is shown in Fig. 48 where the low loss (7 dB) smooth, almost Butterworth, passband and low leakage level (~ 80 dB) are to be noted. The rejection is about 45 dB which is comparable with other devices. The coupling components were varied (this being the real advantage of the three section board) until this response was obtained. The fact that inductors were used (~ 200 nanohenry) in the board is not indicative of what we need in a non-sectioned device due to the differences in parasitics. However, the technique does demonstrate that a good response is obtainable and our task now is to find out how to do this in monolithic form.

In summary, we experienced considerable difficulty in producing the D277 filters but we have learned much and believe that we can make the devices more reliably in the future. There are still design problems to be overcome such as how to acceptably match/couple the filter sections monolithically, to achieve the desired passband, how to produce the 60 dB rejection level, and how to reduce the leakage. We have, however, produced the first six-pole SAW resonator filters that we are aware of and for some purposes the response may be acceptable.

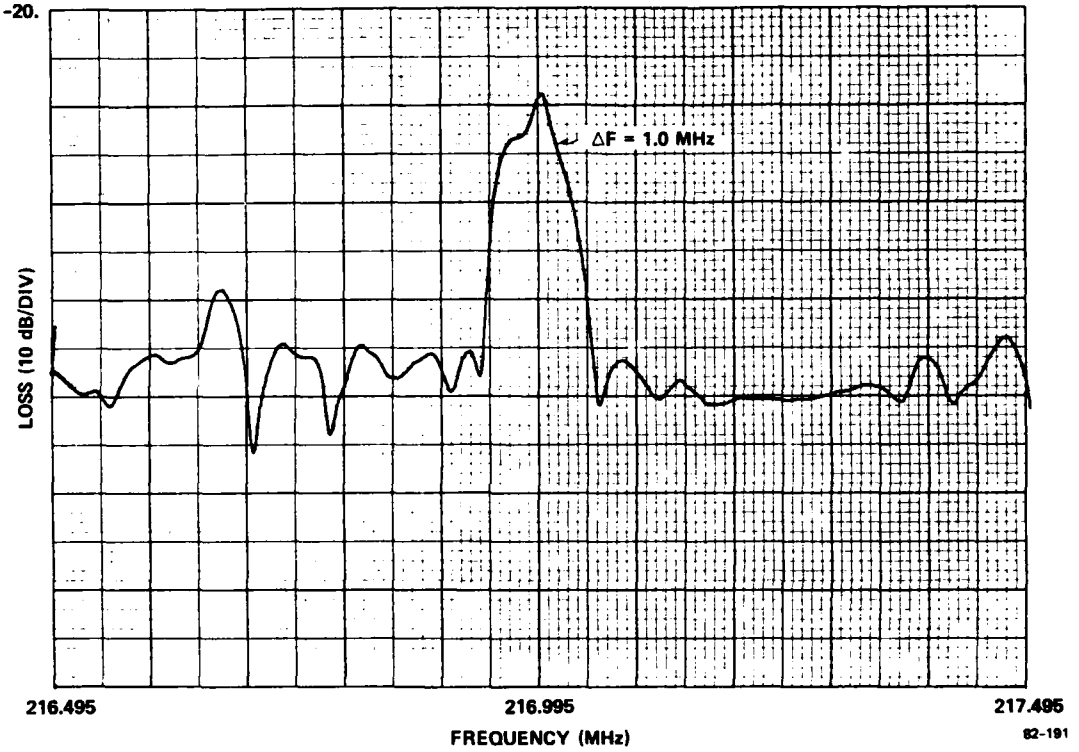

FIG. 46 D277-9 frequency response, unmatched, in air.

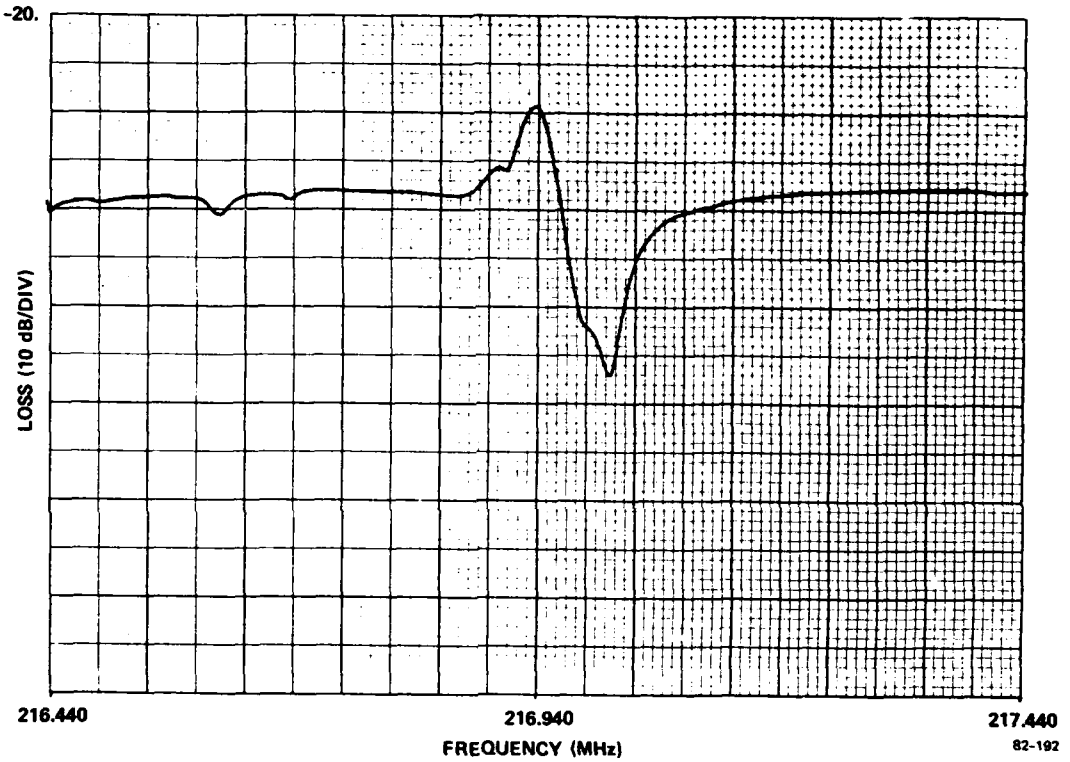

FIG. 47 D277-11 frequency response, unmatched, in air.

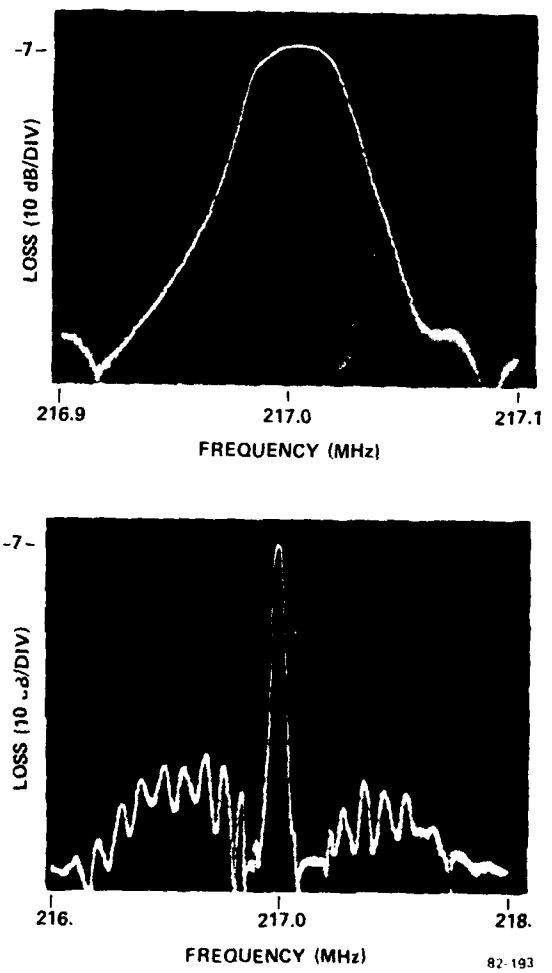

FIG. 48 D277-6 frequency response. Each filter section was in a separate header and inductors (≈ 200 nh) were used to couple cavities 2 to 3 and 4 to 5.

SECTION 5

DISCUSSION AND RECOMMENDATIONS

The work performed to date has been thoroughly discussed in the proceeding sections and we shall now summarize the results noting the problems which remain and presenting recommendations for phase II of this effort.

The out-of-band rejection did not meet specifications because the acoustic singles produced higher sidelobe levels than predicted (by about 20 dB) and the leakage level is relatively strong at about -70 dB on average. The discrepancy in acoustic signal levels may result from the fact that the model does not calculate the response for weighted transducers. We did not include transducer weighting in our model because we did not initially believe it was necessary and the analyses are more time consuming. However, using straightforward analysis techniques we can include weighted transducers and be more accurate than we are at present. We can model leakage, by placing a capacitor between various sections of the filter, but this may not be particularly helpful in tracking down the source of the leakage. Thus we must experimentally try different configurations to see which might decrease the leakage acceptably. Reflector weighting may be possible for the Type I filter since it is smaller. However, to be successful the coupling reflector must also be doubly weighted and this requires some development work.

None of the filters delivered had passband shapes which were the same as predicted. This is due mostly not having the precisely required matching/coupling circuits, but frequency inaccuracies and variations in loss level also contribute. The first thing we must do is to ensure ourselves that we are using an accurate value of electro-acoustic coupling constant (k^2) which we now believe is $k^2 = .0011$. The ability to conveniently vary the coupling components, in particular, is valuable and we have attempted to design the filters so that miniature variable

capacitors could be placed on the substrate and adjusted as required. We were not successful in doing this for D279 and D277. The use of the interdigital capacitors on the substrate shall work ultimately if the capability for adjusting these (laser trimming for instance) exists. We will continue to trim the devices to frequency with care and patience to be as accurate as possible. However, the devices must be bonded and mounted after being trimmed and these processing steps may cause undesireable changes. Virtually anything we try after a device is assembled is destructive so determining the source of inadequate performance is difficult. Loss level variations can be a more serious problem than frequency variation because they are difficult to quantify and reduce. Further, processing step such as bonding and mounting can readily increase cavity losses through contamintion, crystal damage, or other mechanisms. In a research environment these can sometimes be difficult to control.

The package (Type D header) we have chosen to use is basically acceptable for a monolithic filter, however, we must implement a more suitable mounting scheme. We plan to bond the crystal to three mounts (small, flexible structure such as bellows or "C" shaped metal pieces about 0.1" high) which are themselves bonded to the header. The leakage level is to some extent package dependent so we must maintain flexibility on this issue in case we find there is no way to reduce leakage further with the present header. We may also wish to implement a quasi-monolithic structure in which each filter section is produced separately and the three sections bonded to a quartz carrier for mounting in the Type D header. The advantage of this approach is that we should have a higher fabrication yield since one defective section in the monolithic scheme presently used destroys the filter. A third approach, though much less desireable from the point of view of volume required, is to mount each filter section in its own header, and place all three sections on a suitable board with matching/coupling components. This latter scheme has the flexibility we presently (but may not later) need to adjust the coupling values, and it may allow reducing the leakage significantly.

We have produced two different filter designs only one of which used two-port single-pole sections. Carrying through the complete development

of two difference designs, though there is a great deal of overlap, is time consuming and the question we must decide now is whether we think we can continue this dual development and still achieve the desired results. From the point of view of general SAW filter development we believe that the dual-development is desireable since many filter designs will advantageously use both the single-pole and the two-pole sections. However, the additional effort required to carry through the dual-development, including production of five devices of each type for delivery, will more than likely decrease the overall quality of what is done.

Recommendation

In view of the above considerations we recommend the following work be performed in Phase II:

(a) Dual-filter development be continued for the Type I and II requirements. However, the requirement to deliver five devices can be decreased to one for the Type II design since this filter is also under development by SAWTEK Inc.

(b) Synthesis, analysis, and experimental work be pursued to improve the rejection levels.

(c) Investigate techniques for improving the passband response. This include determining k^2 accurately and finding the optimum techniques for section coupling and input/output matching.

(d) Investigate techniques for reducing leakage. The separately-encased three-section configuration should be pursued, in addition to the monolithic single-enclosure scheme, as a back up.

(e) A two-pole filter be made at about 500 MHz and perhaps 800 MHz to demonstrate the feasibility of these devices at higher frequencies.

SECTION 6

SUMMARY

We have successfully produced four- and six-pole SAW resonator filters for the first time, to our knowledge. The foundation for future development work has been established through the successful applicaton of a synthesis technique, development of rapid analysis routines, and the application of our single-pole resonator design and fabrication techniques to multipole configurations utilizing transducer and reflector-coupling. Significant and critical innovations during this program include the techniques, through analysis, of determining the correct isolated-pole resonance frequency to effect a synchronously tuned filter, establishment of physical methods for determining and setting these frequencies, and the establishment of a technqiue for adjusting the coupling of a reflector-coupler. The response characteritics attained thus far meet only some of the performance criteria; notably: insertion loss, shape factor, bandwidths, and center frequencies. Problems remain in shaping the passband, improving the rejection level, and reducing leakage. We have outlined the work to be performed in phase II which is oriented towards solving these problems.

References

1. R. L. Rosenberg and L. A. Coldren, "Scattering analysis and design of SAW Resonator filters," IEEE Trans. on Sonics and Ultrasonics, Vol. SU-26, pp 205-230, May 1979.

2. G. S. Matthaei, E. B. Savage and F. Barman, "Synthesis of SAW resonator filters using any of various coupling mechanisms," IEEE Trans. on Sonics and Ultrasonics, Vol. SU-26, pp. 72-84, March 1978.

3. W. J. Tanski, "Surface acoustic wave resonators on quartz," IEEE Trans. Sonics and Ultrasonics, Vol. SU-26, pp. 93-104, March 1979.

4. A. I. Zvrev, "Handbook of Filter Synthesis," J. Wiley and Sons, New York (1967).

5. "Reference Data for Radio Engineers," Fourth Edition, International Telephone and Telegraph Corp., New York, (1967).

6. Bi-monthly Contract Report No. 1 "Multipole monolithic SAW resonator filters" for Naval Research Lab contract N0014-81-C-2066 (Sperry Research Report No. SRC-CR-81-18, March 1981).

7. W. J. Tanski, "High Q and GHz SAW Resonators," Proc. of the 1978 IEEE Ultrasonics Symposium, pp. 433-437.

8. W. J. Tanski and N. D. Wittels, "SEM observations of SAW resonator transverse modes," Appl. Phys. Lett., 34, No. 9, May 1979, pp. 537-539.

9. W. J. Tanski, "GHz SAW Resonators," Proc. of the 1979 IEEE Ultrasonic Symposium, pp. 815-823.

10. W. J. Tanski, "SAW frequency trimming of resonant and travelling-wave devices on quartz," Appl. Phys. Lett., 39, No. 1, July 1981, pp. 40-42.

11. A. J. Slobodnik, "Surface acoustic waves and SAW materials," IEEE Proc., May 1976, pp. 581-595.

12. R. L. Rosenberg - Bell Telephone Laboratories, Holmdel, NJ - private communication.

13. H. A. Haus, "Modes in SAW grating resonators," Jour. Appl. Phys. 48, No. 12, Dec. 1977, pp. 4955-4961.

14. G. L. Matthaei, L. Young, and E.M.T. Jones, "Microwave Filters, Impedance-Matching Networks, and Coupling Structures," McGraw-Hill, New York, 1964.

15. W. R. Smith, H. M. Gerard, J. H. Collins, T. M. Reeder, and H. J. Shaw, "Analysis of interdigital surface wave transducers by use of an equivalent circuit model," IEEE Trans. Microwave Theory Tech., vol. MTT-17, pp. 856-864, Nov. 1969.

16. M. E. Field, R. C. Ho, and C. L. Chen, "Surface acoustic wave grating reflectors," Proc. 1975 Ultrasonics Symposium, pp. 430-433, (IEEE Cat. No. 75 CH9004-4SU).

17. R. C. M. Li and J. Melngailis, "The influence of stored energy at step discontinuities on the behavior of surface-wave gratings," IEEE Trans. on Sonics and Ultrason, vol. SU22,pp. 189-198, May 1975.

18. "Thin Film Processes" edited by J. L. Vossen and W. Kern (Acedemic Press, New York, 1978).

19. "PLASMOD" etcher/stripper manufactured by Tegal Corp., Sunnyvale, California.

20. Thinco Div. (Hull Corp.) Hatboro, PA 09040 - Series C chip inductors.

21. Available from - United Glass-to-Metal Seals Inc., Chelmsford, MA 01824.

22. "EPO-TEK H44" available from Epoxy Technology Inc., Billerica, MA 01821.

23. Adel Nibbler (Adel Tool Co., Chicago, IL).

24. Johanson Giga-Trim No. 7295 capacitor; Johanson Mfg. Corp., Boonton, NJ 07005.

Susceptance slope parameters ($b_{j,j+1}$) and inverter parameters ($J_{j,j+1}$) for given reflector length (N_g-grooves) and reflectivity (r).

		$J_{j,j+1}$	$b_{j,j+1}$
r =	1.0045000		
	200.00000	.40734074	121.29803
	210.00000 N_g	.38950781	125.49092
	220.00000	.37240223	129.38603
	230.00000	.35605151	132.99870
	240.00000	.34041869	136.34461
	250.00000	.32547224	139.43952
	260.00000	.31116203	142.29902
	270.00000	.29751924	144.93832
	280.00000	.28445634	147.37216
	290.00000	.27196698	149.61470
	300.00000	.26002548	151.67946
	310.00000	.24860926	153.57927
	320.00000	.23769380	155.32625
	330.00000	.22725760	156.93184
	340.00000	.21727961	158.40676
	350.00000	.20773971	159.76105
	360.00000	.19861858	161.00406
	370.00000	.18989811	162.14453
	380.00000	.18156047	163.19057
	390.00000	.17358562	164.14972
	400.00000	.16596722	165.02695
	410.00000	.15868025	165.83472
	420.00000	.15171722	166.57301
	430.00000	.14505209	167.24932
	440.00000	.13866342	167.86875
	450.00000	.13254438	168.43596
	460.00000	.12667268	168.95533
	470.00000	.12103659	169.43076
	480.00000	.11562468	169.86597
	490.00000	.11042683	170.26428
	500.00000	.10543213	170.62879
	510.00000	.10062111	170.96234
	520.00000	.96034254-001	171.26752
	530.00000	.92592642-001	171.54673
	540.00000	.89517702-001	171.80216
	550.00000	.86631236-001	172.03582
	560.00000	.83915411-001	172.24954
	570.00000	.81362733-001	172.44503
	580.00000	.78966030-001	172.62383
	590.00000	.76715480-001	172.78735
	600.00000	.74613509-001	172.93690
	610.00000	.72644865-001	173.07366
	620.00000	.70800563-001	173.19872
	630.00000	.69092879-001	173.31308
	640.00000	.67496343-001	173.41765
	650.00000	.65917722-001	173.51327
	660.00000	.64460016-001	173.60069
	670.00000	.63078442-001	173.68063
	680.00000	.61771428-001	173.75373

N_g	$J_{j,j+1}$	$b_{j,j+1}$
690.00000	.45137604-001	173.82055
700.00000	.43155768-001	173.88165
710.00000	.41260987-001	173.93751
720.00000	.39449379-001	173.98857
730.00000	.37717312-001	174.03527
740.00000	.36061293-001	174.07795
750.00000	.34477983-001	174.11696
760.00000	.32964190-001	174.15265
770.00000	.31516862-001	174.18527
780.00000	.30133060-001	174.21509
790.00000	.28810054-001	174.24235
800.00000	.27545118-001	174.26727
810.00000	.26335720-001	174.29004
820.00000	.25179422-001	174.31087
830.00000	.24073892-001	174.32991
840.00000	.23016902-001	174.34731
850.00000	.22006320-001	174.36322
860.00000	.21040109-001	174.37777
870.00000	.20116720-001	174.39106
880.00000	.19233092-001	174.40322
890.00000	.18388642-001	174.41433
900.00000	.17581269-001	174.42448
910.00000	.16809344-001	174.43377
920.00000	.16071312-001	174.44226
930.00000	.15365654-001	174.45002
940.00000	.14691037-001	174.45711
950.00000	.14046011-001	174.46359
960.00000	.13429306-001	174.46952
970.00000	.12839678-001	174.47494
980.00000	.12275933-001	174.47989
990.00000	.11736950-001	174.48442
1000.0000	.11221626-001	174.48856
1010.0000	.10728928-001	174.49234
1020.0000	.10257863-001	174.49580
1030.0000	.98074908-002	174.49896
1040.0000	.93765728-002	174.50185
1050.0000	.89651712-002	174.50449
1060.0000	.85715457-002	174.50690
1070.0000	.81952027-002	174.50911
1080.0000	.78353835-002	174.51113
1090.0000	.74913526-002	174.51297
1100.0000	.71624462-002	174.51466
1110.0000	.68479713-002	174.51620
1120.0000	.65473038-002	174.51761
1130.0000	.62598373-002	174.51890
1140.0000	.59849924-002	174.52008
1150.0000	.57222149-002	174.52115
1160.0000	.54709749-002	174.52213
1170.0000	.52307658-002	174.52304
1180.0000	.50011034-002	174.52386
1190.0000	.47815246-002	174.52461
r = 1.0050000		
200.00000	.36079717	117.16399
210.00000 N_g	.35085442	120.70254
220.00000	.33376463	123.95054
230.00000	.31754532	126.92735
240.00000	.30209608	129.65201
250.00000	.28739848	132.14294
260.00000	.27341595	134.41782

N_n	$J_{j,j+1}$	$b_{j,j+1}$
270.00000	.26011370	136.49347
280.00000	.24745963	138.38577
290.00000	.23541926	140.10966
300.00000	.22396562	141.67906
310.00000	.21306923	143.10704
320.00000	.20270297	144.40561
330.00000	.19284135	145.58595
340.00000	.18345994	146.65837
350.00000	.17453325	147.63237
360.00000	.16604153	148.51669
370.00000	.15796360	149.31933
380.00000	.15027934	150.04765
390.00000	.14296699	150.70831
400.00000	.13601135	151.30753
410.00000	.12939412	151.85088
420.00000	.12309863	152.34348
430.00000	.11710961	152.79001
440.00000	.11141218	153.19471
450.00000	.10599175	153.56145
460.00000	.10083503	153.89375
470.00000	.95929196-001	154.19481
480.00000	.91262042-001	154.46755
490.00000	.86821955-001	154.71459
500.00000	.82597557-001	154.93830
510.00000	.78579329-001	155.14102
520.00000	.74756282-001	155.32455
530.00000	.71119235-001	155.49076
540.00000	.67659137-001	155.64126
550.00000	.64367360-001	155.77754
560.00000	.61235774-001	155.90093
570.00000	.58256527-001	156.01265
580.00000	.55422226-001	156.11379
590.00000	.52725921-001	156.20536
600.00000	.50160600-001	156.28827
610.00000	.47720164-001	156.36332
620.00000	.45398499-001	156.43126
630.00000	.43189767-001	156.49276
640.00000	.41088496-001	156.54844
650.00000	.39089455-001	156.59883
660.00000	.37187673-001	156.64445
670.00000	.35378416-001	156.68575
680.00000	.33657162-001	156.72313
690.00000	.32019691-001	156.75696
700.00000	.30461967-001	156.78758
710.00000	.28979834-001	156.81530
720.00000	.27569905-001	156.84040
730.00000	.26228572-001	156.86311
740.00000	.24952498-001	156.88366
750.00000	.23738507-001	156.90227
760.00000	.22583560-001	156.91911
770.00000	.21484842-001	156.93435
780.00000	.20439560-001	156.94814
790.00000	.19445133-001	156.96063
800.00000	.18499067-001	156.97193
810.00000	.17599069-001	156.98216
820.00000	.16742837-001	156.99142
830.00000	.15928264-001	156.99980
840.00000	.15153321-001	157.00739
850.00000	.14416050-001	157.01425

N_g	$J_{j,j+1}$	$b_{j,j+1}$
860.00000	.13714708-001	157.02046
870.00000	.13047459-001	157.02608
880.00000	.12412673-001	157.03117
890.00000	.11808771-001	157.03578
900.00000	.11234250-001	157.03995
910.00000	.10687681-001	157.04372
920.00000	.10167703-001	157.04714
930.00000	.96730231-002	157.05023
940.00000	.92024106-002	157.05302
950.00000	.87546943-002	157.05556
960.00000	.83287603-002	157.05785
970.00000	.79235480-002	157.05992
980.00000	.75380519-002	157.06180
990.00000	.71713101-002	157.06350
1000.0000	.68224110-002	157.06504
1010.0000	.64904966-002	157.06643
1020.0000	.61747110-002	157.06769
1030.0000	.58742966-002	157.06883
1040.0000	.55885018-002	157.06986
1050.0000	.53166096-002	157.07079
1060.0000	.50579456-002	157.07164
1070.0000	.48118661-002	157.07240
1080.0000	.45777568-002	157.07309
1090.0000	.43550414-002	157.07372
1100.0000	.41431576-002	157.07429
1110.0000	.39415804-002	157.07480
1120.0000	.37498200-002	157.07527
1130.0000	.35673335-002	157.07568
1140.0000	.33936229-002	157.07607
1150.0000	.32282065-002	157.07641
1160.0000	.30706232-002	157.07672
1170.0000	.29204824-002	157.07700
1180.0000	.27774121-002	157.07726
1190.0000	.26410568-002	157.07749
r = 1.0055000		
200.00000	.33327517	112.65954
210.00000	.31605549	115.62489
220.00000	.29916657	118.31482
230.00000	.28321858	120.75156
240.00000	.26810255	122.95623
250.00000	.25379330	124.94674
260.00000	.24024776	126.74793
270.00000	.22742519	128.37106
280.00000	.21528698	129.83436
290.00000	.20379662	131.15260
300.00000	.19291952	132.33965
310.00000	.18262296	133.40780
320.00000	.17287595	134.36573
330.00000	.16364917	135.23270
340.00000	.15491483	136.00926
350.00000	.14664607	136.70703
360.00000	.13881980	137.33382
370.00000	.13141067	137.89670
380.00000	.12439698	138.40209
390.00000	.11775762	138.85575
400.00000	.11147203	139.26291
410.00000	.10552308	139.62827
420.00000	.99891067-001	139.95608
430.00000	.94559650-001	140.25015

440.00000	.69513763-001	140.51394
450.00000	.64735279-001	140.75453
460.00000	.60212762-001	140.96271
470.00000	.75931422-001	141.15298
480.00000	.71678976-001	141.32359
490.00000	.69042629-001	141.47656
500.00000	.64411033-001	141.61371
510.00000	.60973272-001	141.73657
520.00000	.57718983-001	141.84690
530.00000	.54636742-001	141.94571
540.00000	.51722215-001	142.03428
550.00000	.48961661-001	142.11362
560.00000	.46345464-001	142.18484
570.00000	.43874758-001	142.24863
580.00000	.41533061-001	142.30580
590.00000	.39316346-001	142.35704
600.00000	.37217942-001	142.40297
610.00000	.35231534-001	142.44413
620.00000	.33351146-001	142.48102
630.00000	.31571119-001	142.51406
640.00000	.29886095-001	142.54371
650.00000	.28291005-001	142.57026
660.00000	.26781049-001	142.59406
670.00000	.25351663-001	142.61538
680.00000	.23998605-001	142.63449
690.00000	.22717744-001	142.65162
700.00000	.21505246-001	142.66697
710.00000	.20357461-001	142.68073
720.00000	.19270937-001	142.69305
730.00000	.18242432-001	142.70410
740.00000	.17268763-001	142.71399
750.00000	.16347090-001	142.72287
760.00000	.15474608-001	142.73081
770.00000	.14648692-001	142.73794
780.00000	.13866858-001	142.74432
790.00000	.13126752-001	142.75004
800.00000	.12426147-001	142.75517
810.00000	.11762935-001	142.75976
820.00000	.11135119-001	142.76388
830.00000	.10540813-001	142.76757
840.00000	.99782251-002	142.77087
850.00000	.94456641-002	142.77384
860.00000	.89415273-002	142.77649
870.00000	.84642974-002	142.77887
880.00000	.80125383-002	142.78100
890.00000	.75848936-002	142.78291
900.00000	.71800575-002	142.78462
910.00000	.67966508-002	142.78615
920.00000	.64340872-002	142.78753
930.00000	.60909851-002	142.78876
940.00000	.57656112-002	142.78987
950.00000	.54576873-002	142.79085
960.00000	.51665972-002	142.79174
970.00000	.48908346-002	142.79254
980.00000	.46297995-002	142.79325
990.00000	.43826964-002	142.79388
1000.0000	.41487518-002	142.79446
1010.0000	.39273517-002	142.79497
1020.0000	.37177399-002	142.79543

N_g	$J_{j,j+1}$	$h_{j,j+1}$
1030.0000	.35193185-002	142.79584
1040.0000	.33314215-002	142.79621
1050.0000	.31536727-002	142.79654
1060.0000	.29853539-002	142.79683
1070.0000	.28260167-002	142.79710
1080.0000	.26751676-002	142.79735
1090.0000	.25324066-002	142.79755
1100.0000	.23972463-002	142.79774
1110.0000	.22692997-002	142.79791
1120.0000	.21481819-002	142.79806
1130.0000	.20335285-002	142.79820
1140.0000	.19249944-002	142.79833
1150.0000	.18222530-002	142.79844
1160.0000	.17249959-002	142.79853
1170.0000	.16329282-002	142.79862
1180.0000	.15457751-002	142.79870
1190.0000	.14632735-002	142.79877
r = 1.0000000		
200.00000	.30227629	108.00644
210.00000	.28472413	110.47793
220.00000	.26819118	112.69413
230.00000	.25261823	114.67685
240.00000	.23794956	116.45428
250.00000	.22413264	118.04093
260.00000	.21111502	119.45765
270.00000	.19885912	120.72170
280.00000	.18731205	121.84678
290.00000	.17643548	122.85315
300.00000	.16619047	123.74772
310.00000	.15654336	124.54414
320.00000	.14745059	125.25298
330.00000	.13887264	125.88340
340.00000	.13078355	126.44414
350.00000	.12317736	126.94269
360.00000	.11602197	127.38585
370.00000	.10930207	127.77968
380.00000	.10299353	128.12961
390.00000	.97003624-001	128.44049
400.00000	.91370954-001	128.71662
410.00000	.86065356-001	128.96187
420.00000	.81067834-001	129.17965
430.00000	.76360502-001	129.37303
440.00000	.71926503-001	129.54473
450.00000	.67749382-001	129.69716
460.00000	.63815972-001	129.83248
470.00000	.60110396-001	129.95260
480.00000	.56619991-001	130.05922
490.00000	.53332261-001	130.15386
500.00000	.50235439-001	130.23785
510.00000	.47318439-001	130.31239
520.00000	.44570819-001	130.37855
530.00000	.41982743-001	130.43726
540.00000	.39544949-001	130.48936
550.00000	.37246709-001	130.53559
560.00000	.35085903-001	130.57662
570.00000	.33043491-001	130.61303
580.00000	.31129472-001	130.64534
590.00000	.29321995-001	130.67400
600.00000	.27619273-001	130.69944

510.00000	.26015516-001	130.72201
520.00000	.24504584-001	130.74204
530.00000	.23081969-001	130.75981
540.00000	.21741675-001	130.77558
550.00000	.20479213-001	130.78950
560.00000	.19290055-001	130.80196
570.00000	.18169947-001	130.81299
580.00000	.17114981-001	130.82277
590.00000	.16121078-001	130.83144
700.00000	.15184932-001	130.83915
710.00000	.14303242-001	130.84595
720.00000	.13472702-001	130.85201
730.00000	.12690383-001	130.85736
740.00000	.11953500-001	130.86215
750.00000	.11259401-001	130.86638
760.00000	.10605606-001	130.87014
770.00000	.99897751-002	130.87347
780.00000	.94097080-002	130.87646
790.00000	.88633137-002	130.87904
800.00000	.83486517-002	130.88137
810.00000	.78636737-002	130.88343
820.00000	.74072454-002	130.88526
830.00000	.69771320-002	130.88689
840.00000	.65719938-002	130.88833
850.00000	.61908905-002	130.88961
860.00000	.58309702-002	130.89074
870.00000	.54923443-002	130.89175
880.00000	.51734226-002	130.89264
890.00000	.48730196-002	130.89343
900.00000	.45900600-002	130.89414
910.00000	.43235300-002	130.89476
920.00000	.40724762-002	130.89531
930.00000	.38360033-002	130.89581
940.00000	.36132597-002	130.89624
950.00000	.34034501-002	130.89663
960.00000	.32056234-002	130.89697
970.00000	.30196721-002	130.89728
980.00000	.28443301-002	130.89755
990.00000	.26791696-002	130.89779
1000.0000	.25235993-002	130.89800
1010.0000	.23770625-002	130.89819
1020.0000	.22390747-002	130.89835
1030.0000	.21091216-002	130.89850
1040.0000	.19866579-002	130.89863
1050.0000	.18712053-002	130.89875
1060.0000	.17623507-002	130.89885
1070.0000	.16596055-002	130.89895
1080.0000	.15625030-002	130.89903
1090.0000	.14708965-002	130.89910
1100.0000	.13844603-002	130.89916
1110.0000	.13029009-002	130.89922
1120.0000	.12258136-002	130.89927
1130.0000	.11529329-002	130.89932
1140.0000	.10840027-002	130.89935
1150.0000	.10187823-002	130.89939
1160.0000	.95744439-003	130.89942
1170.0000	.91277529-003	130.89945
1180.0000	.85977355-003	130.89948
1190.0000	.80984944-003	130.89950

	N_g	$J_{j,j+1}$	$b_{j,j+1}$
1.000e000			
200.00000		.27366034	103.35321
210.00000		.25651969	105.40446
220.00000		.24041854	107.22304
230.00000		.22533577	108.83343
240.00000		.21119923	110.25600
250.00000		.19794954	111.51709
260.00000		.18553109	112.62904
270.00000		.17389170	113.61041
280.00000		.16298253	114.47602
290.00000		.15275774	115.23913
300.00000		.14317441	115.91160
310.00000		.13419230	116.50394
320.00000		.12577308	117.02555
330.00000		.11788321	117.48472
340.00000		.11048775	117.88883
350.00000		.10355625	118.24439
360.00000		.97056597-001	118.55719
370.00000		.90970513-001	118.83231
380.00000		.85263439-001	119.07425
390.00000		.79914397-001	119.28700
400.00000		.74900930-001	119.47404
410.00000		.70201965-001	119.63846
420.00000		.65797530-001	119.78302
430.00000		.61669971-001	119.91007
440.00000		.57801977-001	120.02173
450.00000		.54174899-001	120.11986
460.00000		.50772211-001	120.20610
470.00000		.47579741-001	120.28189
480.00000		.44583114-001	120.34846
490.00000		.41768791-001	120.40699
500.00000		.39124022-001	120.45841
510.00000		.36725793-001	120.50359
520.00000		.34421783-001	120.54328
530.00000		.32262317-001	120.57815
540.00000		.30237825-001	120.60879
550.00000		.28341309-001	120.63571
560.00000		.26563304-001	120.65936
570.00000		.24896842-001	120.68014
580.00000		.23334927-001	120.69839
590.00000		.21871000-001	120.71443
600.00000		.20499812-001	120.72852
610.00000		.19212963-001	120.74090
620.00000		.18007573-001	120.75177
630.00000		.16877859-001	120.76132
640.00000		.15819019-001	120.76971
650.00000		.14826605-001	120.77706
660.00000		.13896451-001	120.78350
670.00000		.13024459-001	120.78925
680.00000		.12207543-001	120.79425
690.00000		.11441697-001	120.79864
700.00000		.10723896-001	120.80250
710.00000		.10051126-001	120.80588
720.00000		.94205654-002	120.80886
730.00000		.88295619-002	120.81147
740.00000		.82759351-002	120.81377
750.00000		.77564592-002	120.81579
760.00000		.72698541-002	120.81756
770.00000		.68137768-002	120.81912

AD-A115 468 SPERRY RESEARCH CENTER SUDBURY MA F/G 9/5
MULTIPOLE MONOLITHIC SURFACE ACOUSTIC WAVE (SAW) RESONATOR FILT--ETC(U)
APR 82 N00014-81-C-2066
UNCLASSIFIED SRC-CR-82-19 NL

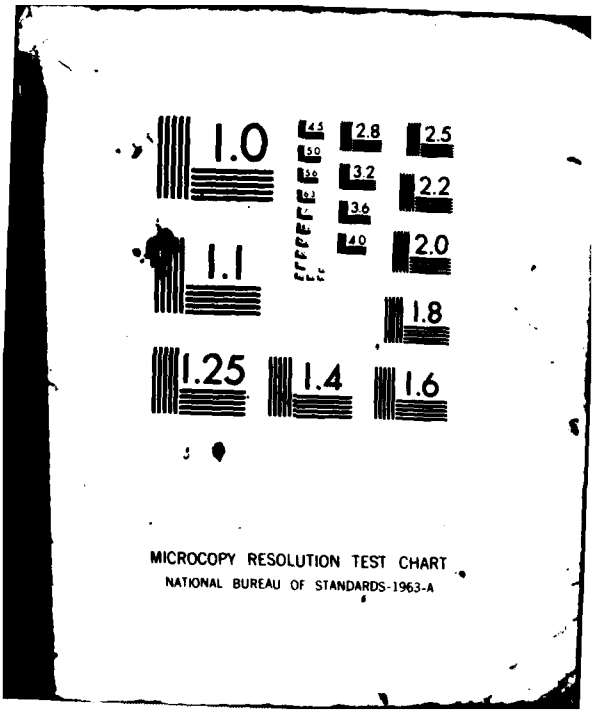
1.0
1.1
1.25
1.4
1.6
2.8
2.5
3.2
2.2
3.6
2.0
4.0
1.8
MICROCOPY RESOLUTION TEST CHART
NATIONAL BUREAU OF STANDARDS-1963-A

N_g	$J_{j,j+1}$	$b_{j,j+1}$
780.00000	.63063109-002	120.82046
790.00000	.59356626-002	120.82169
800.00000	.56101492-002	120.82274
810.00000	.52991939-002	120.82367
820.00000	.49831866-002	120.82449
830.00000	.46191362-002	120.82520
840.00000	.43293544-002	120.82583
850.00000	.40577503-002	120.82638
860.00000	.38031854-002	120.82687
870.00000	.35645907-002	120.82729
880.00000	.33409645-002	120.82767
890.00000	.31313675-002	120.82800
900.00000	.29349196-002	120.82829
910.00000	.27507961-002	120.82854
920.00000	.25782236-002	120.82876
930.00000	.24164775-002	120.82896
940.00000	.22649767-002	120.82913
950.00000	.21227904-002	120.82928
960.00000	.19896161-002	120.82941
970.00000	.18647966-002	120.82953
980.00000	.17478077-002	120.82963
990.00000	.16381582-002	120.82972
1000.0000	.15353876-002	120.82980
1010.0000	.14390643-002	120.82987
1020.0000	.13487839-002	120.82993
1030.0000	.12641473-002	120.82999
1040.0000	.11848592-002	120.83003
1050.0000	.11105265-002	120.83008
1060.0000	.10408571-002	120.83011
1070.0000	.97555842-003	120.83014
1080.0000	.91435629-003	120.83017
1090.0000	.85699372-003	120.83020
1100.0000	.80322981-003	120.83022
1110.0000	.75283861-003	120.83024
1120.0000	.70560911-003	120.83025
1130.0000	.66134239-003	120.83027
1140.0000	.61985276-003	120.83028
1150.0000	.58096601-003	120.83029
1160.0000	.54451683-003	120.83030
1170.0000	.51035818-003	120.83031
1180.0000	.47834062-003	120.83032
1190.0000	.44837170-003	120.83033
r = 1.6070000		
200.00000 N_g	.24780230	98.798031
210.00000	.23110567	100.49491
220.00000	.21553404	101.98256
230.00000	.20101160	103.29541
240.00000	.18746766	104.42532
250.00000	.17483632	105.42187
260.00000	.16305606	106.29251
270.00000	.15206953	107.05266
280.00000	.14182326	107.71607
290.00000	.13226737	108.29474
300.00000	.12335535	108.79932
310.00000	.11504381	109.23914
320.00000	.10729229	109.62242
330.00000	.10006306	109.95633
340.00000	.93320930-001	110.24717
350.00000	.87023074-001	110.50045

360.00000	.61165957-001	110.72099
370.00000	.75699522-001	110.91299
380.00000	.70599256-001	111.08012
390.00000	.65842361-001	111.22559
400.00000	.61405979-001	111.35219
410.00000	.57268516-001	111.46237
420.00000	.53409830-001	111.55825
430.00000	.49811137-001	111.64167
440.00000	.46454921-001	111.71426
450.00000	.43324843-001	111.77741
460.00000	.40405665-001	111.83235
470.00000	.37683178-001	111.88015
480.00000	.35144130-001	111.92174
490.00000	.32776159-001	111.95791
500.00000	.30567740-001	111.98936
510.00000	.28506121-001	112.01675
520.00000	.26587277-001	112.04057
530.00000	.24795957-001	112.06126
540.00000	.23125141-001	112.07930
550.00000	.21566996-001	112.09496
560.00000	.20113837-001	112.10861
570.00000	.18758590-001	112.12047
580.00000	.17494658-001	112.13078
590.00000	.16315885-001	112.13975
600.00000	.15216543-001	112.14756
610.00000	.14191270-001	112.15434
620.00000	.13235079-001	112.16025
630.00000	.12343314-001	112.16539
640.00000	.11511636-001	112.16985
650.00000	.10735995-001	112.17374
660.00000	.10012617-001	112.17712
670.00000	.93379782-002	112.18006
680.00000	.87097961-002	112.18261
690.00000	.81220076-002	112.18484
700.00000	.75747561-002	112.18677
710.00000	.70643778-002	112.18845
720.00000	.65893883-002	112.18992
730.00000	.61444704-002	112.19119
740.00000	.57304631-002	112.19230
750.00000	.53443512-002	112.19326
760.00000	.49842550-002	112.19410
770.00000	.46494217-002	112.19483
780.00000	.43352164-002	112.19546
790.00000	.40431146-002	112.19601
800.00000	.37706943-002	112.19649
810.00000	.35166293-002	112.19691
820.00000	.32796829-002	112.19727
830.00000	.30587017-002	112.19759
840.00000	.28526099-002	112.19786
850.00000	.26604044-002	112.19810
860.00000	.24811494-002	112.19831
870.00000	.23139725-002	112.19849
880.00000	.21580597-002	112.19864
890.00000	.20126521-002	112.19878
900.00000	.18770420-002	112.19890
910.00000	.17505691-002	112.19900
920.00000	.16326178-002	112.19909
930.00000	.15226139-002	112.19917
940.00000	.14200219-002	112.19924


ATE
LME